DOI: 10.1111/mpp.13166

ORIGINAL ARTICLE

Molecular Plant Pathology WILEY

Nitrate-inducible MdBT2 acts as a restriction factor to limit apple necrotic mosaic virus genome replication in *Malus domestica*

Zhenlu Zhang | Yin-Huan Xie | Ping Sun | Fu-Jun Zhang | Peng-Fei Zheng | Xiao-Fei Wang | Chun-Xiang You | Yu-Jin Hao†

State Key Laboratory of Crop Biology, College of Horticulture Science and Engineering, Shandong Agricultural University, Tai'an, China

Correspondence
Zhenlu Zhang and Chun-Xiang You, State Key Laboratory of Crop Biology, College of Horticulture Science and Engineering, Shandong Agricultural University, Tai'an 271000, China.
Emails: zzhenlu0526@sdau.edu.cn; youchunxiang@sdau.edu.cn

Abstract

Apple necrotic mosaic virus (ApNMV) is highly associated with the occurrence of apple mosaic disease in China. However, ApNMV–host interactions and defence mechanisms of host plants against this virus are poorly studied. Here, we report that nitrate treatment restrains ApNMV genomic RNA accumulation by destabilizing viral replication protein 1a through the MdBT2-mediated ubiquitin-proteasome pathway. MdBT2, a nitrate-responsive BTB/TAZ domain-containing protein, was identified in a yeast two-hybrid screen of an apple cDNA library using viral protein 1a as bait, and 1a was further confirmed to interact with MdBT2 both in vivo and in vitro. It was further verified that MdBT2 promoted the ubiquitination and degradation of viral protein 1a through the ubiquitin-proteasome pathway in an MdCUL3A-independent manner. Viral genomic RNA accumulation was reduced in *MdBT2*-overexpressing transgenic apple leaves but enhanced in *MdBT2*-antisense leaves compared to the wild type. Moreover, MdBT2 was found to interfere with the interaction between viral replication proteins 1a and $2a^{pol}$ by competitively interacting with 1a. Taken together, our results demonstrate that nitrate-inducible MdBT2 functions as a limiting factor in ApNMV viral RNA accumulation by promoting the ubiquitination and degradation of viral protein 1a and interfering with interactions between viral replication proteins.

KEYWORDS

ApNMV, *Malus domestica*, MdBT2, ubiquitination, viral genomic RNA replication, virus–host interactions

Abbreviations: ApNMV, apple necrotic mosaic virus; BiFC, bimolecular fluorescence complementation; BMV, brome mosaic virus; Co-IP, co-immunoprecipitation; CRL, cullin-RING ligase; MET, methyltransferase; MP, movement protein; RdRp, RNA-dependent RNA polymerase; UPS, ubiquitin proteasome system; VRC, viral replication complex; Y2H, yeast two-hybrid.

†Deceased.

1 | INTRODUCTION

Apple mosaic disease is a major and widely distributed viral disease that affects apple tree growth and production all over the world. The causal agent of this disease was traditionally believed to be apple mosaic virus (ApMV), which belongs to the genus *Ilarvirus* in the family *Bromoviridae* (Bujarski et al., 2012). However, recent studies have revealed that apple necrotic mosaic virus (ApNMV), rather than ApMV, is highly associated with the occurrence of apple mosaic disease in China (Noda et al., 2017; Xing et al., 2018), where half of the world's apples are produced.

Like ApMV, ApNMV is an ilarvirus, and both viruses share a common genomic structure (Noda et al., 2017). They have three positive-sense single-stranded genomic RNAs (RNA1, RNA2, and RNA3) and an encapsidated subgenomic RNA4 derived from RNA3 (Noda et al., 2017). RNA1 encodes the 1a protein, which is characterized by an N-terminal methyltransferase (MET) domain and a C-terminal NTP-binding helicase (HEL) domain. RNA2 encodes the viral RNA-dependent RNA polymerase (RdRp, $2a^{pol}$). The movement protein (MP) is encoded by the RNA3, and the coat protein (CP) is encoded by the subgenomic RNA4 (Bujarski et al., 2012). Based on the well-characterized model virus brome mosaic virus (BMV), which belongs to the same family as ApNMV, 1a is a multifunctional protein that plays essential roles in virus replication. It induces the formation of the viral replication complex (VRC), recruits $2a^{pol}$ and template RNAs into the VRCs, and facilitates viral genomic RNA replication (Diaz & Wang, 2014).

In natural environments, plants face continuous biotic and abiotic stresses that compromise their survival. To counteract these environmental challenges, plants have evolved various complex and efficient mechanisms of resistance, including the ubiquitin proteasome system (UPS) that is highly conserved among eukaryotes (Adams & Spoel, 2018; Zhou & Zeng, 2017). The UPS is an enzymatic process in which ubiquitin moieties are covalently conjugated to substrate proteins for degradation by the proteasome, and this process has been demonstrated to play key roles in many intracellular biological processes of plants (Alcaide-Loridan & Jupin, 2012; Bachmair et al., 2001; Vierstra, 2009). The ubiquitination process is mediated by a series of enzymes: a ubiquitin-activating enzyme (E1), a ubiquitin-conjugating enzyme (E2), and a ubiquitin E3 ligase (E3). E3 ensures targeting specificity by interacting with target substrates and transferring ubiquitin from E2 to the target, thereby generating the ubiquitin modification (Metzger et al., 2014). Based on their composition and activation mechanisms, four main types of E3 ligases are found in plants: HECT (homologous to E3 associated protein C-terminus), RING (really interesting new gene), U-box, and CRLs (cullin-RING ligases) (Mazzucotelli et al., 2006; Vierstra, 2009). CRLs are the most abundant E3 ligases in plants. They exist as complexes with a cullin (CUL) subunit that serves as a molecular scaffold, and three types of CUL (CUL1, CUL3, and CUL4) have been reported in various plants (Hotton & Callis, 2008).

The BTB (bric-a-brac, tramtrack, and broad complex)-type E3 ligases are one of the CRL subfamilies (Vierstra, 2009). In CUL3-RING E3 ligases (CRL3) of the model plant *Arabidopsis thaliana*, BTB/POZ (poxvirus and zinc finger) domain-containing proteins interact directly with both the CUL3 and the target substrate, and thus serve as the substrate receptor to select proteins for degradation via the UPS (Genschik et al., 2013; Hua & Vierstra, 2011). BTB/POZ domain-containing proteins play critical roles in multiple intracellular processes. For instance, the BTB-BACK domain protein POB1 regulates plant immunity by interacting with and targeting PUB (Plant U-box) 17 and PUB29 for degradation in *Nicotiana benthamiana* (Orosa et al., 2017) and apple (*Malus domestica*) (Han et al., 2019), respectively. In *Arabidopsis*, AtBT2 contains an N-terminal BTB/POZ domain, a central TAZ (transcriptional adaptor zinc finger) domain, and a C-terminal calmodulin-binding domain (Ren et al., 2007). AtBT2 has been reported to participate in the regulation of multiple responses. It responds to circadian rhythms, light, stresses, and nutrients, suppresses sugar signalling, modulates plant hormone responses by suppressing abscisic acid (ABA) signalling while enhancing auxin signalling, and regulates telomerase activity by acting downstream of TAC1 (TELOMERASE ACTIVATOR1) (Kunz et al., 2015; Mandadi et al., 2009; Misra et al., 2018; Ren et al., 2007). MdBT2, a homolog of AtBT2, has been shown to function as a signal hub to regulate anthocyanin biosynthesis, leaf senescence, iron homeostasis, and malate accumulation in response to multiple hormonal and environmental signals (An, Zhang, et al., 2019; An, Wang, et al., 2020; Zhao et al., 2016; Zhang, Gu, Cheng, et al., 2020; Zhang, Gu, Wang, et al., 2020). For example, MdBT2 interacts with and promotes the ubiquitination and degradation of MdMYB1 and MdCIbHLH1 (cold-induced basic helix-loop-helix1) to inhibit the accumulation of anthocyanin (Wang et al., 2018) and malate (Zhang, Gu, Cheng, et al., 2020; Zhang, Gu, Wang, et al., 2020), respectively, in response to nitrate. In addition, MdBT2 functions to delay leaf senescence by interacting with and promoting the ubiquitination and degradation of MdbHLH93 (basic helix-loop-helix93) and MdMYC2 (myelocytomatosis protein2) in apple (An, Zhang, et al., 2019; An et al., 2021).

Nitrogen (N) is a major nutrient for plant growth and productivity. It has also been reported to play key roles in plant immunity by regulating plant resistance to various pathogens (Dordas, 2008). A well-known defence-related N derivative is nitric oxide (NO), which is partially generated by nitrate reductase (NR), a key enzyme in nitrate assimilation. Multiple lines of evidence have demonstrated the roles of NO in transcriptional regulation of defence genes that encode pathogen-related (PR) proteins or proteins involved in phytoalexin synthesis, posttranslational protein modifications, and salicylic acid (SA) accumulation (reviewed in Wendehenne et al., 2014). For example, NO functions in brassinosteroid-mediated resistance to viral infection in *N. benthamiana* (tobacco mosaic virus, TMV) (Deng et al., 2016) and *A. thaliana* (cucumber mosaic virus, CMV) (Zou et al., 2018). In addition, nitrate, an inorganic nitrogen form that is usually taken up by roots from aerobic soil, was also proved to be involved in disease resistance. For example, application of a NO_3^- efflux inhibitor delays and reduces the hypersensitive cell death triggered by cryptogein in tobacco, and this is accompanied by suppressed

induction of some defence-related genes (Wendehenne et al., 2002). Moreover, feeding tobacco plants with NO_3^- enhances the accumulation of SA and the expression of the *PR1* gene, as well as the speed of cell death on infection by *Pseudomonas syringae* pv. *phaseolicola* (Gupta et al., 2013). All these reports reveal the potential role of nitrogen in resistance against pathogens.

In this study, we found that the nitrate-responsive protein MdBT2 interacted with ApNMV protein 1a, promoting its ubiquitination and degradation through the 26S proteasomal pathway in an MdCUL3A-independent manner. ApNMV genomic RNA accumulation was inhibited in transgenic apples overexpressing *MdBT2* (*MdBT2*-OE) but enhanced in transgenic apples expressing an antisense RNA against *MdBT2* (*MdBT2*-anti) compared to that in the wild type (WT). In addition, MdBT2 interfered with the interaction between 1a and $2a^{pol}$ by competitively interacting with 1a.

2 | RESULTS

2.1 | Nitrate treatment decreases ApNMV viral RNA accumulation

In addition to being a critical nutrient for plant growth and development, nitrate also functions as an important signalling molecule to regulate the expression of multiple genes in response to various environmental factors (Ho et al., 2009; Scheible et al., 2004) and to regulate plant resistance to pathogens (Dordas, 2008; Gupta et al., 2013; Wendehenne et al., 2002). To determine whether nitrate has any effect on ApNMV infection, we first constructed an infectious clone for ApNMV by inserting the full length of ApNMV RNA1, RNA2, and RNA3 into binary vectors driven by the double CaMV 35S promoter (Figure 1a). The recombinant constructs were then introduced into *Agrobacterium tumefaciens* separately and co-transformed into apple plantlet leaves under different nitrate concentrations via the vacuum method. Viral RNA accumulation of infected leaves was tested by northern blotting using digoxygenin (DIG)-labelled probes targeting the CP coding sequence. We found that RNA levels decreased with increasing concentrations of KNO_3 (Figure 1b). When the concentration of KNO_3 increased to 10 mM, (+)RNA3 accumulation decreased to about 20% compared to that observed without KNO_3 (Figure 1b). Similar results were obtained from reverse transcription quantitative PCR (RT-qPCR) testing: increased concentration of KNO_3 dramatically inhibited ApNMV viral genomic RNA accumulation in locally infected leaves (Figure 1c). These data suggest that high nitrate levels inhibited ApNMV viral genomic RNA replication.

2.2 | Nitrate treatment destabilizes viral 1a protein through the UPS pathway

Based on the model virus BMV, replication proteins play key roles in viral genomic RNA duplication. We thus hypothesized that nitrate treatment might decrease the protein stability of the two presumed replication proteins of ApNMV, 1a and $2a^{pol}$, to compromise its replication. To verify our hypothesis, we used western blotting and a cell-free protein degradation assay to test the effect of nitrate on the protein stability of the two viral replication proteins both in vivo and in vitro. Using an anti-1a specific antibody, we found that 1a protein accumulation decreased with increasing concentrations of KNO_3 (Figure 2a), which might be a reason that the viral genomic RNA accumulation was reduced on nitrate treatment (Figure 1b,c). We next used a cell-free degradation system to test the effect of nitrate on the protein stability of 1a and $2a^{pol}$ in vitro. Increased transcript levels of two representative nitrate-responsive genes, *MdNRT1.1* (Ho et al., 2009) and *MdBT2* (An, Wang, et al., 2020; Wang et al., 2018), under KNO_3 treatment confirmed that the apple plantlets indeed responded to nitrate (Figure S1). Next, we mixed equal amounts of 1a-HIS or $2a^{pol}$-HIS fusion proteins obtained from a prokaryotic expression system with total proteins extracted from GL3 leaves treated with KNO_3 or KCl and incubated the mixtures for different times. Western blot analysis showed that the 1a-HIS protein degraded more rapidly in proteins extracted from KNO_3-treated GL3 leaves than in those from KCl-treated leaves (Figure 2b). By contrast, the rates of $2a^{pol}$-HIS protein degradation were similar in proteins extracted from KCl- and KNO_3-treated leaves (Figure S2a), suggesting that nitrate treatment compromised the protein stability of 1a but not $2a^{pol}$. Interestingly, we also observed that 1a was also weakly degraded in KCl-treated apple leaves (Figure 2b) and callus (Figure S2b) in vitro, indicating that, in addition to the nitrate-induced UPS pathway, 1a might undergo protein degradation through some other mechanisms, such as the autophagy-lysosome pathway, sumoylation, and phosphorylation, that need to be verified.

UPS-mediated protein degradation is one of the most common and powerful protein degradation pathways in plants. To determine whether nitrate-induced 1a-HIS protein degradation is dependent on the proteasome pathway, the proteasome inhibitor MG132 was applied and dimethyl sulphoxide (DMSO) served as a control. Total proteins extracted from KNO_3-treated GL3 leaves were pretreated with MG132 or DMSO for 30 min, 1a-HIS fusion protein was added to the samples, and protein degradation was measured as described above. The addition of MG132 largely inhibited 1a-HIS protein degradation, whereas DMSO had no effect (Figure 2c). We also included HIS protein (a HIS tag protein obtained from pET-32a empty vector through the prokaryotic expression system) as a negative control, which cannot be degraded by nitrate treatment (Figure S3a). MdMYB1-HIS was included as a positive control, which can be induced to degradation by nitrate treatment (Figure S3b, left panel) (Wang et al., 2018), and addition of MG132 inhibited the degradation of MdMYB1-HIS induced by nitrate (Figure S3b, right panel). Collectively, these data suggested that KNO_3-induced 1a-HIS protein degradation was most probably mediated by the proteasome pathway.

We also performed a cell-free degradation assay using protein extracts from KNO_3- or KCl-treated apple calli to further confirm the nitrate-mediated induction of 1a-HIS protein (Figure S2b,c). Results with apple calli were similar to those obtained with apple leaves.

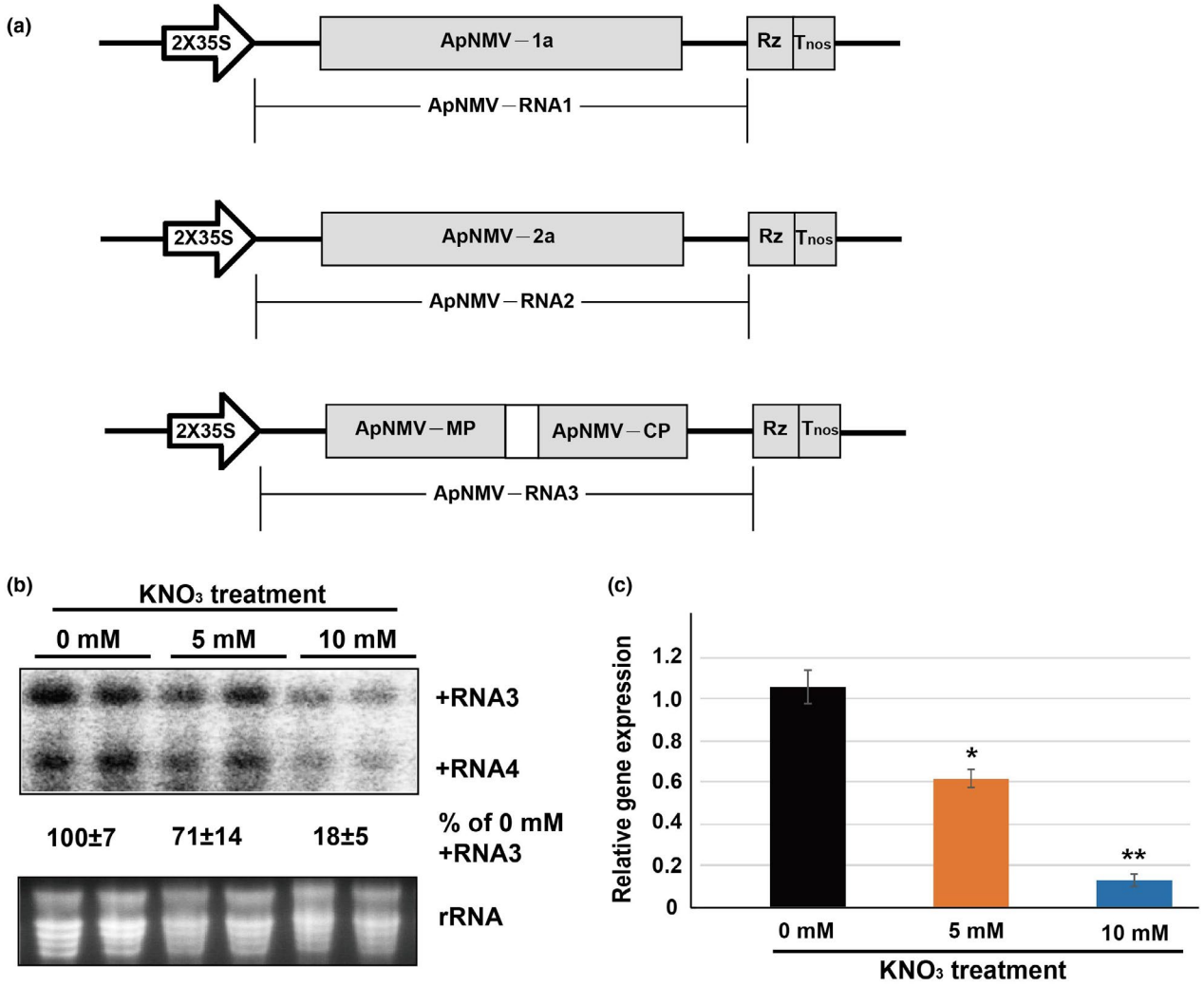

FIGURE 1 Nitrate treatment inhibits ApNMV viral RNA accumulation in *Malus domestica*. (a) Schematic model of the ApNMV infectious clone construction. The three RNA segments were inserted into binary vectors. In the constructs, the three segments were driven by the double CaMV 35S promoter and were followed by a ribozyme (Rz) and a Nos terminator (Tnos). (b) Northern blotting was used to measure ApNMV RNA accumulation in leaves of apple (GL3) treated with KNO_3. The infectious clone of ApNMV was used to agro-infiltrate GL3 leaves with the indicated concentrations of KNO_3, and the leaves were collected for RNA extraction 4 days after infiltration. Digoxygenin (DIG)-labelled probes targeting the coat protein (CP) coding sequence were used to measure the RNA levels of (+)RNA3 and (+)RNA4 in a northern blot assay with two replicates for each treatment. The values (mean ± *SD*) indicate the signal intensity of (+)RNA3 and the band intensity of 0 mM KNO_3 was set to 100. The rRNA served as a loading control. (c) Reverse transcription quantitative PCR (RT-qPCR) was used to measure ApNMV RNA accumulation in leaves of GL3 treated with KNO_3. Primers targeting the CP-coding sequence were used for the RT-qPCR test and *MdACTIN* served as the housekeeping gene. Bars indicate mean values of the relative transcript levels of the ApNMV CP-coding gene. The mean values were calculated from nine repeats, for which the whole experiments were repeated three times with three technical replicates each time. Error lines within the bars indicate *SD* of the nine repeats. The mean value of 0 mM KNO_3 was set to 1.0. Significant difference was analysed between different KNO_3 concentrations compared with 0 mM. $^*p < 0.05$, $^{**}p < 0.01$ (based on single factor analysis of variance test). The experiment was repeated three times

We concluded that nitrate treatment inhibits ApNMV genomic RNA replication by destabilizing viral protein 1a through the UPS pathways.

2.3 | ApNMV 1a interacts with MdBT2

The UPS is a complex enzymatic process and many host factors are involved in this pathway. Given that nitrate inhibits ApNMV genomic RNA replication by degrading viral protein 1a through the UPS pathway (Figures 1 and 2), we next performed a yeast two-hybrid (Y2H) assay using 1a protein as bait to screen an apple cDNA library to determine the protein(s) that mediate the degradation of ApNMV 1a under nitrate treatment. MdBT2 (MDP0000643281), a known nitrate-responsive protein, was identified as a potential prey. This protein contains an N-terminal BTB domain, a BACK-like domain in the middle, and a C-terminal TAZ domain (Figure 3a). A Y2H assay was performed to confirm the protein interaction between ApNMV 1a and MdBT2. The coding sequences of 1a and MdBT2

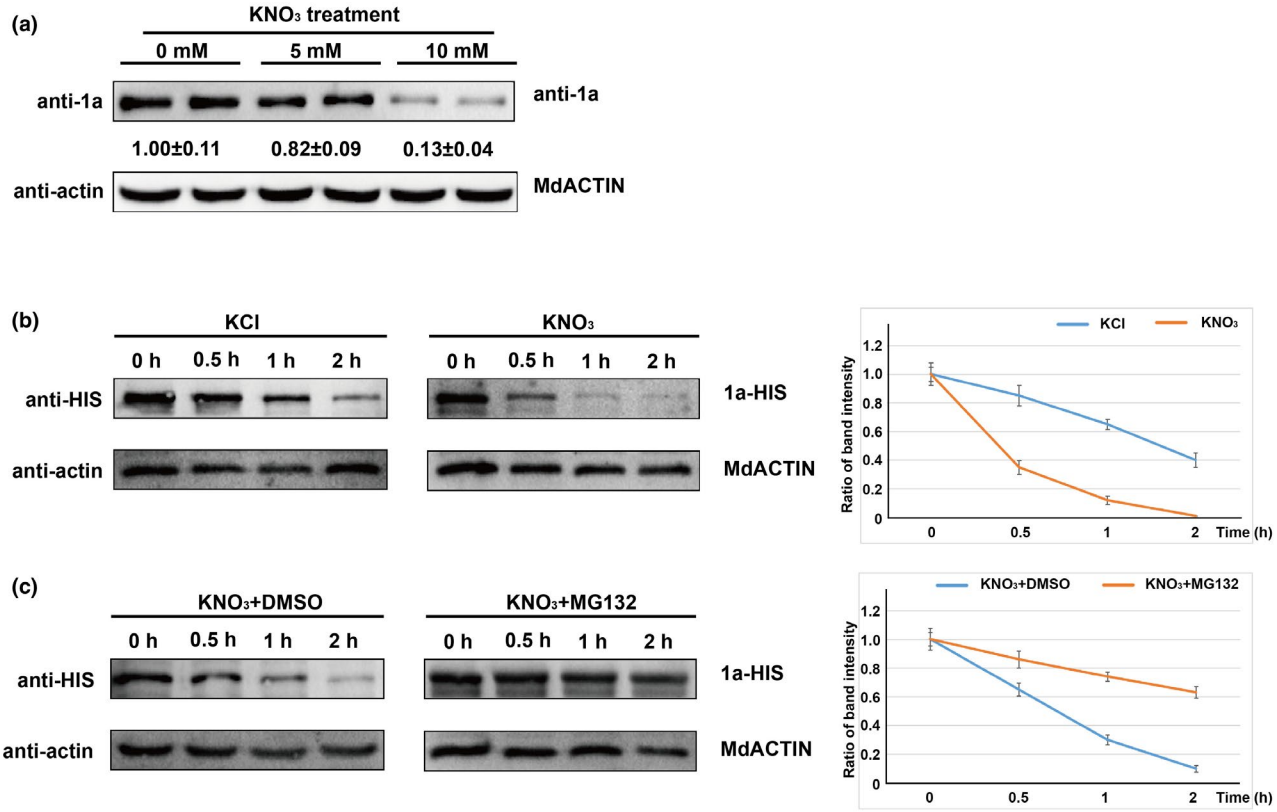

FIGURE 2 Nitrate treatment destabilizes viral protein 1a through the UPS pathways. (a) Protein levels of 1a in leaves of apple (GL3) treated with KNO_3. The infectious clone of ApNMV was used to agro-infiltrate GL3 leaves under the indicated concentrations of KNO_3, and the leaves were collected for protein extraction 4 days after infiltration. Anti-1a specific antibody was used in a western blot assay with two replicates of each treatment. MdACTIN served as a loading control. The values (mean ± *SD*) indicate the signal intensity and the band intensity of 0 mM KNO_3 was set to 1.0. (b) 1a-HIS protein degradation in a cell-free degradation assay. The same amount (100 ng) of 1a-HIS protein obtained from prokaryotic expression was incubated with total proteins extracted from apple callus treated with KCl or KNO_3 at the indicated time points. The protein samples were then collected and the reactions were stopped by addition of SDS-PAGE loading buffer and boiled for 5 min. All the prepared samples were subjected to western blot detection with anti-HIS antibody. MdACTIN served as a loading control. (c) 1a-HIS protein degradation in proteins extracted from KNO_3-pretreated apple callus in the presence or absence of proteasome inhibitor MG132. The samples were collected at the indicated time points and subjected to western blot detection with anti-HIS antibody. MdACTIN served as a loading control. The charts on the right side show the degradation trends in (b) (upper chart) and (c) (bottom chart), respectively. Bars indicate signal intensity values of means ± *SD*. The ordinate shows the ratio of band intensity at each time point compared to that at 0 h. The intensity of the protein bands at 0 h was set to 1.0. All experiments were repeated independently three times

were inserted into pGBT9 and pGAD424, respectively, and then co-transformed into yeast cells. The colonies grew normally on SD/−Trp/−Leu/−His/−Ade defective medium, suggesting that there was an interaction between 1a and MdBT2 (Figure S4). We also tested interactions between MdBT2 and other viral components ($2a^{pol}$, MP, and CP) using Y2H assays, and found that MdBT2 interacted only with 1a and not with the other viral proteins (Figure S4).

To identify the domain(s) that is(are) required for interaction between the two proteins, we first divided MdBT2 into several fragments based on its domain distribution (Figure 3a) and inserted them into pGBD vectors. Full-length MdBT2 served as a positive control. Yeast grew on SD/−Trp/−Leu/−His/−Ade defective medium only when both BACK-like and TAZ domains were present, indicating that two domains are responsible for the interaction with 1a (Figure 3a). We next divided 1a into the N-terminal MET domain and the C-terminal HEL domain and found that neither of them interacted alone with MdBT2 (Figure 3b), indicating that both the N-terminal MET domain and the C-terminal HEL domain of 1a are required for the interaction with MdBT2.

We next used a bimolecular fluorescence complementation (BiFC) assay to verify the 1a–MdBT2 interaction. *Agrobacterium* harbouring MdBT2-nYFP and 1a-cYFP constructs were co-infiltrated into *N. benthamiana* leaves, and strong yellow fluorescence signals were observed in the cytoplasm under a confocal microscope (Figure 3c, upper panel). However, the combinations of MdBT2-nYFP with cYPF (Figure 3c, middle panel) and 1a-cYFP with nYFP (Figure 3c, bottom panel) produced no fluorescence signal. These data indicated that ApNMV 1a physically interacted with MdBT2 in the cytoplasm in vivo.

We performed a pull-down assay to further confirm the interaction between 1a and MdBT2. The fusion protein glutathione S-transferase (GST)-1a or GST tag protein fused with nothing was incubated with MdBT2-HIS and glutathione (GSH)-attached beads. The target proteins were eluted with GSH solution and tested with

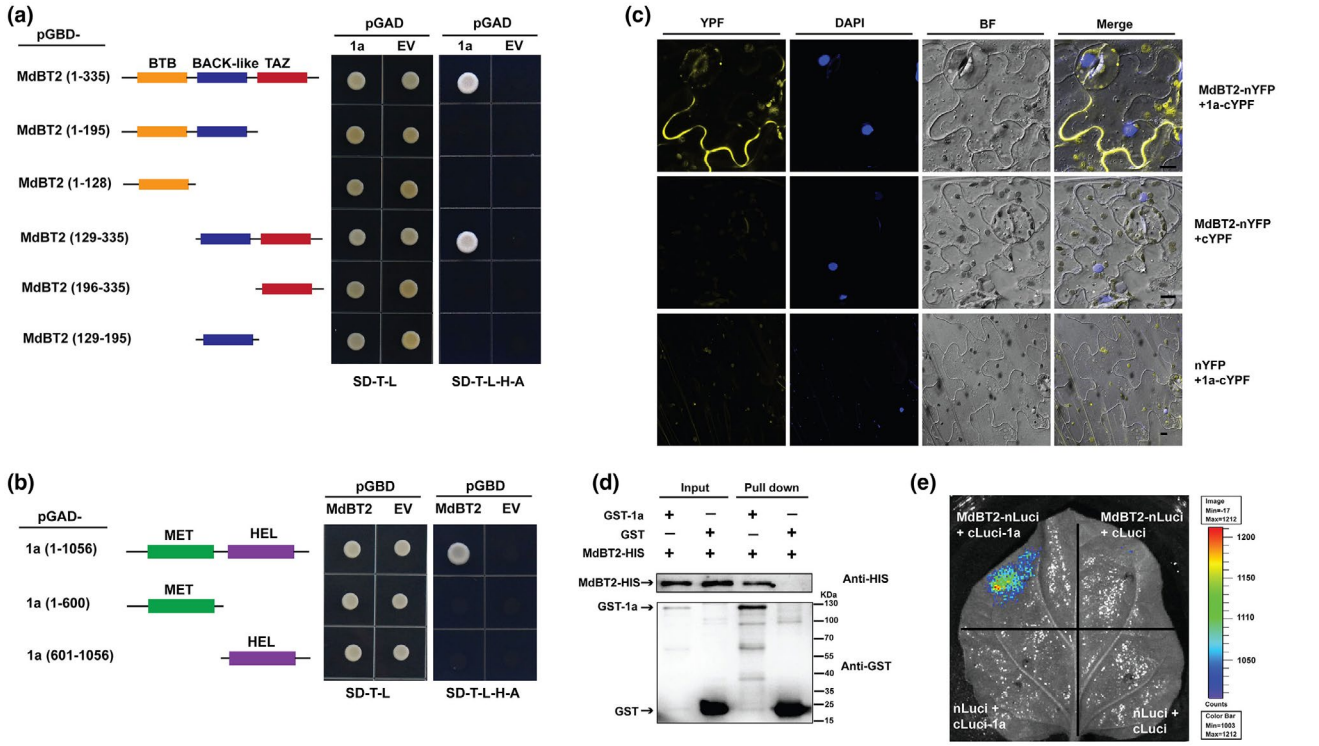

FIGURE 3 MdBT2 interacts with ApNMV 1a in vivo and in vitro. (a) and (b) illustrate the interactions between MdBT2 and 1a. MdBT2 (a) and 1a (b) were divided into different fragments based on their domain structures, and different colours on the left side indicate the different domains that were included in the assay. Different combinations of constructs were transformed into yeast cells and cultured on selective medium SD−Trp/−Leu (SD−T−L). Interactions were tested on selective medium SD−Trp/−Leu/−His−Ade (SD−T−L−H−-A). The images were taken 3 days after incubation at 28°C. (c) A bimolecular fluorescence complementation (BiFC) assay demonstrated the interaction of MdBT2 with 1a in *Nicotiana benthamiana* cells. The nuclei were stained with 4′,6-diamidino-2-phenylindole (DAPI). YFP, yellow fluorescent protein; BF, bright field; scale bar, 10 μm. (d) A pull-down assay demonstrated the in vitro interaction between MdBT2 and 1a. MdBT2-HIS protein was incubated with GST-1a or glutathione S-transferase (GST) protein and passed through a glutathione (GSH)-attached column. Anti-GST and anti-HIS antibodies were used to detect the target proteins. GST-1a, GST, and MdBT2-HIS bands are indicated by arrows on the left side. The ladder on the right side indicates the molecular mass (kDa) of the target proteins. (e) Luciferase complementation imaging assays demonstrated the interaction between MdBT2 and 1a in *N. benthamiana* cells. The bar on the right side indicates the intensity of the captured signals. Empty nLuci and cLuci vectors served as controls. Representative images of three independent experiments are shown here

anti-GST and anti-HIS antibodies. MdBT2-HIS fusion protein was pulled down in the presence of GST-1a but not GST (Figure 3d), suggesting that GST-1a interacted with MdBT2-HIS in vitro.

Finally, we confirmed the 1a–MdBT2 interactions using a luciferase complementation imaging assay. *Agrobacterium* harbouring MdBT2-nLuci and cLuci-1a were co-infiltrated into *N. benthamiana* leaves, and empty vectors served as the control. Luminescent signals were observed only when both MdBT2-nLuci and cLuci-1a were present, and no signal was captured with the combinations of MdBT2-nLuci plus cLuci combination or nLuci plus cLuci-1a (Figure 3e), suggesting that 1a and MdBT2 interacted in vivo. Collectively, these data indicated that ApNMV 1a interacts with MdBT2 both in vivo and in vitro.

2.4 | MdBT2 promotes ubiquitination and degradation of ApNMV 1a

Given that MdBT2 is one of the components of the BTB/POZ type E3 ligase and functions in the interaction with target proteins, we therefore hypothesized that MdBT2 might promote the ubiquitination and degradation of its interacting partner ApNMV 1a. To verify our hypothesis, we first performed a cell-free degradation assay using WT, *MdBT2*-OE (overexpression), and *MdBT2*-anti (antisense) apple calli. *MdBT2* expression was increased in the overexpression callus but inhibited in the antisense callus compared to the WT (Figure S5a), suggesting that these calli were suitable for use in MdBT2 functional analysis. Total protein extracts from the three callus types were incubated with 1a-HIS fusion protein for different time periods. After immunoblotting with anti-HIS antibody, we found 1a-HIS protein degraded more rapidly in proteins extracted from *MdBT2*-OE transgenic callus (Figure 4a, the middle section) and more slowly in protein extracts from *MdBT2*-anti callus (Figure 4a, the right section) compared to those from the WT (Figure 4a, left section). These data indicate that MdBT2 promotes 1a protein degradation in vitro. To test whether the proteasome is involved in 1a-HIS degradation, we performed these experiments with the proteasome inhibitor MG132, and 1a-HIS protein degradation was inhibited in proteins from all three types of callus (Figure 4b), suggesting that

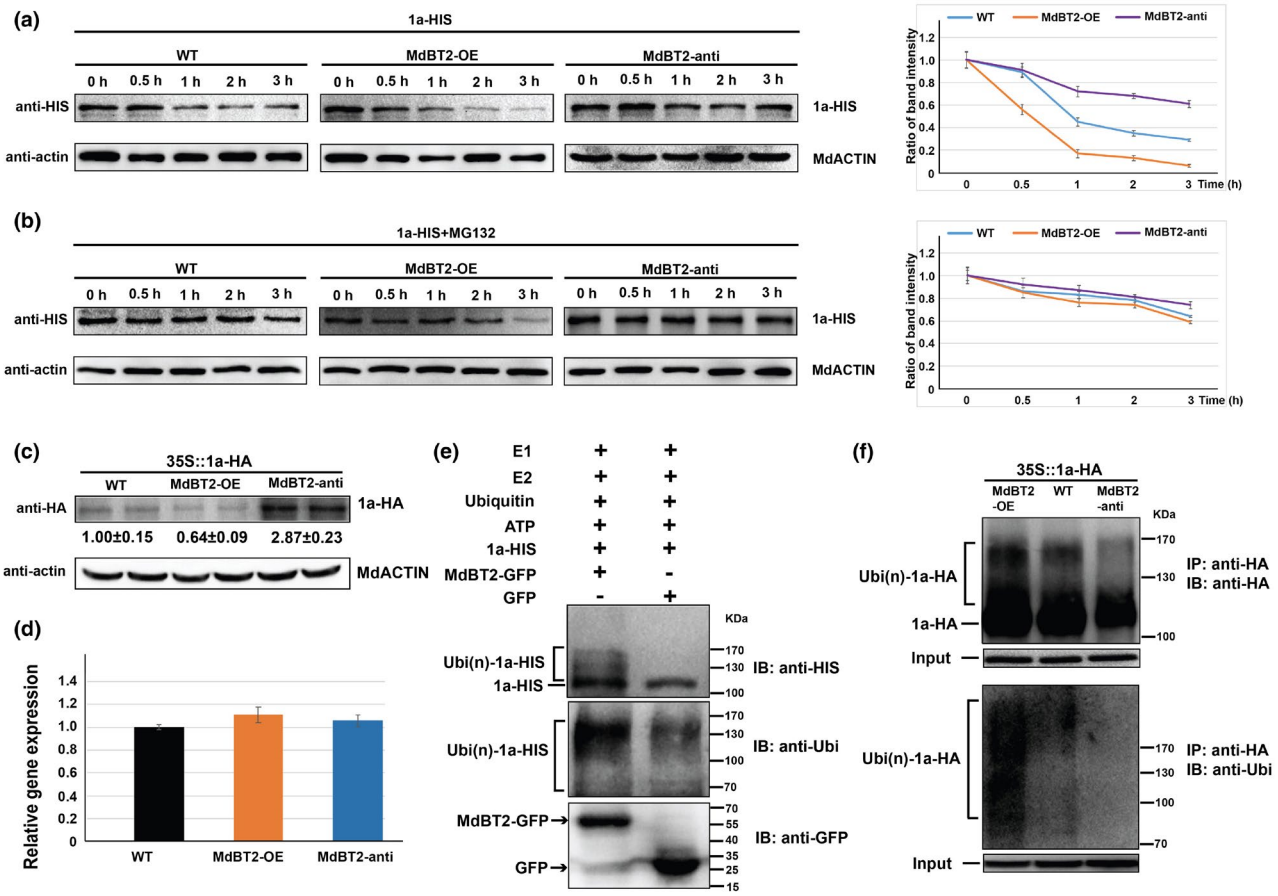

FIGURE 4 MdBT2 promotes the ubiquitination and degradation of 1a in vivo and in vitro. 1a protein degradation in total proteins extracted from different transgenic apple calli in the absence (a) or presence (b) of the proteasome inhibitor MG132 in a cell-free protein degradation assay. 1a-HIS protein was incubated with protein extracts from transgenic (*MdBT2*-OE [overexpression] and *MdBT2*-anti [antisense]) and wild-type (WT) apple calli for the indicated times. Anti-HIS was used to detect the target proteins. MdACTIN served as a loading control. The charts on the right side show the protein degradation trends in (a) (upper chart) and (b) (lower chart). The ordinate shows the ratio of band intensity at each time point compared to that at 0 h and the intensity of the protein bands at 0 h was set to 1.0. The *35S::1a-HA* construct was transiently expressed in WT, *MdBT*-OE, and *MdBT2*-anti apple (GL3) leaves, and the leaves were collected for protein (c) and RNA (d) extraction 5 days after agro-infiltration. Anti-HA antibody was used to detect the 1a-HA protein in a western blot assay (c). MdACTIN served as a loading control in the western assay. (d) Reverse transcription quantitative PCR was used to measure the transcript level of 1a in *35S::1a-HA* transiently expressed in WT, *MdBT*-OE, and *MdBT2*-anti apple leaves. Bars indicate mean values of relative transcript levels of 1a. The mean values were calculated from six repeats, for which the whole experiments were repeated twice with three technical repeats in each time. Error lines with the bars indicate *SD* of the six repeats. Relative 1a transcript level of WT was set to 1.0. (e) MdBT2-mediated 1a protein ubiquitination in vitro. Active MdBT2-GFP protein was immunoprecipitated from *35S::MdBT2-GFP* transgenic apple callus using anti-GFP antibody and incubated with 1a-HIS protein, E1, E2, and ubiquitin in vitro. GFP (green fluorescent protein) immunoprecipitated from *35S::GFP* transgenic apple calli served as a control. Anti-HIS (upper panel) and anti-Ubi (lower panel) antibodies were used to detect the target proteins. Anti-GFP antibody was used to detect the input of GFP and the active MdBT2-GFP proteins. 1a-HIS and Ubi(n)-1a-HIS are labelled on the left side. (f) MdBT2-mediated 1a-HA protein ubiquitination in vivo. A *35S::1a-HA* construct was transiently expressed in WT, *MdBT2*-OE, and *MdBT2*-anti apple leaves, and the samples were collected for protein extraction 4 days after infiltration. Anti-HA antibody was used for immunoprecipitation (IP), and anti-HA (upper panel) and anti-Ubi (lower panel) antibodies were used for immunoblotting (IB). Input indicates the samples collected before IP and detected with anti-Actin antibody. 1a-HA and Ubi(n)-1a-HA are labelled on the left side. Representative images of three independent experiments are shown here

the 26S proteasome pathway may be involved in MdBT2-mediated 1a-HIS protein degradation.

To further verify the role of MdBT2 in promoting ApNMV 1a protein degradation, we transiently transformed *Agrobacterium* harbouring a pCXSN-1a-HA construct into leaves of WT, *MdBT2*-OE, and *MdBT2*-anti apple plantlets using the vacuum method. The transgenic apple plantlets had been generated previously in our laboratory. We confirmed that the *MdBT2*-OE plantlets had a higher *MdBT2* expression level compared to the WT, whereas the *MdBT2*-anti plantlets had lower *MdBT2* expression (Figure S5b), suggesting that these transgenic plantlets were suitable for use in MdBT2 functional analysis. Total proteins were extracted 5 days after transformation, and anti-HA antibody was used for immunoblotting. The 1a-HA protein level in *MdBT2*-OE leaves was lower than that in

WT leaves and higher in *MdBT2*-anti transgenic leaves (Figure 4c). Because the transcript level of 1a-HA was similar among the three types of leaves (Figure 4d), we concluded that MdBT2 regulated the protein stability of 1a-HA in vivo.

We next tested whether ubiquitination was involved in MdBT2-mediated ApNMV 1a protein destabilization. Active MdBT2-GFP proteins were first obtained by immunoprecipitation from total protein extracts of *MdBT2*-OE callus using anti-GFP antibody (Zhang et al., 2020). Then, 1a-HIS protein was incubated with human E1, E2, ubi, and active MdBT2-GFP in incubation buffer, and proteins were detected using anti-HIS and anti-Ubi antibodies. GFP proteins immunoprecipitated from *35S:GFP* transgenic apple callus served as the control. High-molecular mass forms of 1a-HIS (i.e., polyubiquitinated 1a-HIS, Ubi(n)-1a-HIS) were detected in the presence of active MdBT2 protein by immunoblotting with anti-HIS antibody (Figure 4e, upper image). A larger amount of ubiquitinated protein was also detected in the presence of active MdBT2-GFP by immunoblotting with anti-Ubi antibody (Figure 4e, lower image). These data suggest that MdBT2 is involved in promoting the ubiquitination of 1a-HIS in vitro.

To determine whether MdBT2 promotes 1a-HIS protein ubiquitination in vivo, we transformed pCXSN-1a-HA into leaves of WT, *MdBT2*-OE, and *MdBT2*-anti apple plantlets as described above. After treatment with MG132, total protein extracts from the three types of apple leaves were immunoprecipitated with anti-HA antibody, and the precipitates were probed using anti-HA (Figure 4f, upper image) and anti-Ubi (Figure 4f, lower image) antibodies. The amount of Ubi(n)-1a-HA was higher in *MdBT2*-OE leaves and lower in *MdBT2*-anti leaves compared to the WT (Figure 4f), indicating that MdBT2 promoted the ubiquitination of 1a protein in vivo. Therefore, these data indicate that MdBT2 is involved in promoting 1a protein ubiquitination and degradation via the UPS pathways.

2.5 | MdCUL3A is not involved in MdBT2-mediated degradation of ApNMV 1a

In CRL3-type E3 ligase complexes, BTB/POZ proteins usually serve as a scaffold to link the target protein and CUL3 through physical protein interactions (Gingerich et al., 2005; Hua & Vierstra, 2011). Previous reports have demonstrated the interaction between MdBT2 and MdCUL3A (Wang et al., 2018; Zhao et al., 2016), and we reconfirmed this interaction via a pull-down assay. Similar results were obtained: MdCUL3A-HIS protein was pulled down only in the presence of GST-MdBT2, suggesting the physical interaction of the two proteins (Figure S6a).

We next tested whether MdCUL3A was involved in MdBT2-mediated 1a protein degradation. A cell-free degradation assay was performed using total proteins extracted from *MdCUL3A*-OE transgenic apple callus. The transcript level of *MdCUL3A* was higher in *MdCUL3A*-OE callus than in WT apple callus (Figure S6b), suggesting that these transgenic materials were suitable for use in the functional analysis of MdCUL3A. After immunoblotting with anti-HIS antibody, we found that the rate of 1a-HIS protein degradation was similar in the proteins extracted from *MdCUL3A*-OE and WT calli (Figure 5a), suggesting that MdCUL3A may not be closely involved in MdBT2-mediated 1a protein degradation.

To explore the possible reasons for this result, we performed a competitive pull-down assay to test the effect of MdCUL3A on the 1a–MdBT2 interactions. The addition of increased amounts of MdCUL3A-HIS protein decreased the quantity of MdBT2-HIS that was pulled down (Figures 5b and S7a), suggesting that MdCUL3A-HIS represses the interaction between GST-1a and MdBT2-HIS, and this may explain why MdCUL3A had no effect on MdBT2-mediated 1a degradation.

2.6 | MdBT2 suppresses ApNMV genomic RNA accumulation by promoting 1a ubiquitination and degradation

Given that 1a plays critical roles in viral genomic RNA replication of ApNMV (by analogy to the closely related model virus BMV), we hypothesized that MdBT2-mediated 1a degradation might inhibit ApNMV genomic RNA replication in apple. To verify our hypothesis, we transformed the infectious clone of ApNMV into leaves of WT, *MdBT2*-OE, and *MdBT2*-anti apple using the vacuum method. Five days after transformation, the leaves were collected and prepared for extraction of total proteins and RNA. We first tested the protein level of 1a using anti-1a specific antibody and found that it was lower in *MdBT2*-OE leaves and higher in *MdBT2*-anti leaves compared to those of the WT (Figure 6a). This result suggested that MdBT2 promoted the degradation of 1a protein during virus infection. We next verified the MdBT2-mediated ubiquitination of 1a and found that the amount of poly-ubiquitinated 1a was higher in *MdBT2*-OE leaves and lower in *MdBT2*-anti leaves compared to those of the WT when probed with anti-1a antibody (Figure 6b, upper image). Also, more ubiquitinated proteins were present in *MdBT2*-OE leaves and fewer were present in *MdBT2*-anti leaves compared to the WT when probed with anti-Ubi antibody (Figure 6b, lower image), suggesting that MdBT2 promoted ApNMV 1a protein ubiquitination and degradation during virus infection.

We then determined the role of MdBT2 in ApNMV viral RNA replication by northern blotting using a DIG-labelled probe targeting the CP-coding sequence of ApNMV. Accumulated viral RNA levels in *MdBT2*-OE leaves were lower, and higher in *MdBT2*-anti leaves, compared with those of the WT (Figure 6c). RT-qPCR results also demonstrated that viral genomic RNA accumulation significantly increased in *MdBT2*-anti leaves but dramatically decreased in *MdBT2*-OE leaves compared with those of the WT (Figure 6d), suggesting that MdBT2 suppressed ApNMV replication in apple. These data indicate that MdBT2 may repress ApNMV genomic RNA replication by promoting the ubiquitination and degradation of 1a protein.

2.7 | MdBT2 interferes with the interactions between 1a and $2a^{pol}$

We have previously identified a protein interaction between ApNMV 1a and $2a^{pol}$, and their homologs in BMV are both necessary

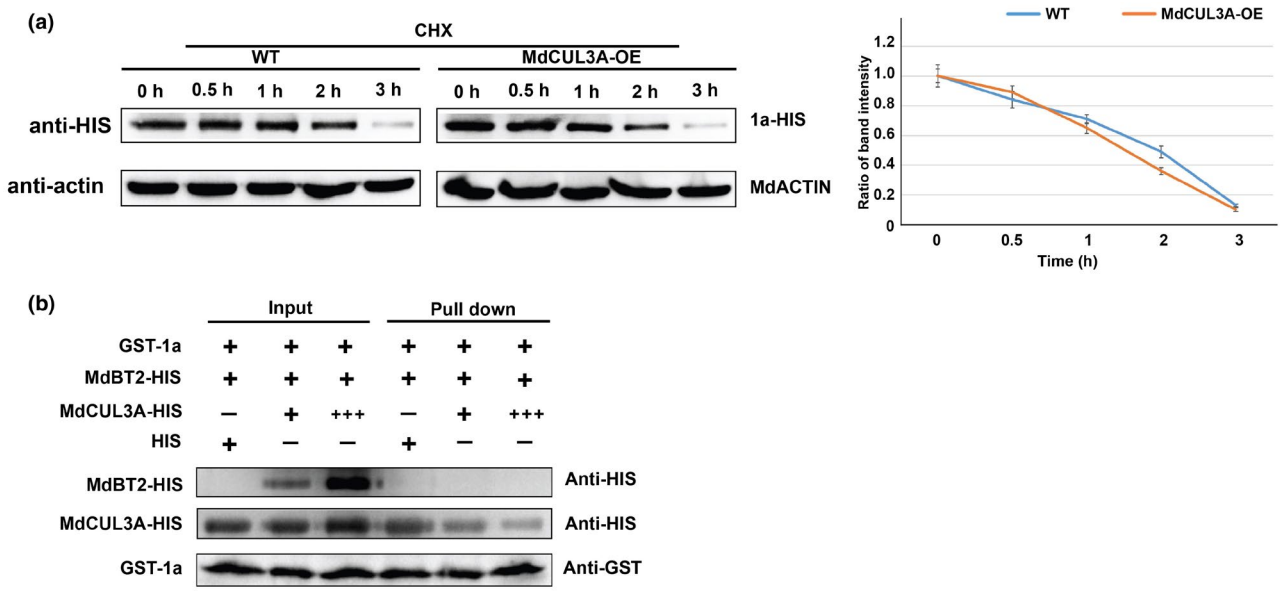

FIGURE 5 MdBT2 promoted 1a degradation by an MdCUL3A-independent pathway. (a) In vitro degradation of 1a-HIS in proteins extracted from *MdCUL3A* overexpression (*MdCUL3A*-OE) and wild-type (WT) apple calli. 1a-HIS protein obtained from a prokaryotic expression system was incubated with protein extracts from WT or *MdCUL3A*-OE for the indicated times in the presence of the translation inhibitor cycloheximide (CHX). MdACTIN served as a loading control. The chart on the right side indicates the protein degradation trend. The ordinate shows the ratio of band intensity at each time point compared to that at 0 h, and protein band intensity at 0 h was set to 1.0. (b) A competitive pull-down assay showed the effect of MdCUL3A-HIS on the interaction between GST-1a and MdBT2-HIS. GST-1a and MdBT2-HIS proteins were incubated with different amounts of MdCUL3A-HIS protein and passed through a glutathione (GSH)-attached column. A simple HIS-tag protein served as a control when MdCUL3A-HIS was absent. For the amount of MdCUL3A-HIS, a single + indicates 2 μg of protein and + + + indicates 6 μg of protein. Anti-HIS antibody was used to detect both the MdCUL3A-HIS and MdBT2-HIS proteins. All the experiments were repeated three times and representative images are shown

and sufficient to support viral genomic RNA replication in that virus (Diaz & Wang, 2014; Zhang, Zhang, et al., 2020). Given that 1a also interacted with MdBT2 (Figure 3), we next asked whether MdBT2 affected the interaction between 1a and $2a^{pol}$. We first performed a luciferase complementation imaging assay to explore the relationships among the three proteins. The interaction between 1a and $2a^{pol}$ was reconfirmed in the assay, and strong luminescent signals were observed only in the presence of both 1a-nLuci and cLuci-$2a^{pol}$ (Figure 7a). Then pCXSN-MdBT2-HA was introduced, co-infiltrated with 1a-nLuci and cLuci-$2a^{pol}$, and observed with an in vivo imaging system. Luminescent signals decreased progressively with an increasing proportion of pCXSN-MdBT2-HA (Figure 7b), suggesting that MdBT2-HA competed with $2a^{pol}$ and interfered with its interactions with 1a in vivo.

To further verify the disruption of 1a–$2a^{pol}$ interactions by MdBT2, we next performed a competitive pull-down assay using GST-$2a^{pol}$, MdBT2-HIS, and 1a-HIS fusion proteins obtained from a prokaryotic expression system. GST-$2a^{pol}$ and 1a-HIS were mixed and incubated with MdBT2-HIS, then passed through a GSH-attached column. The amount of 1a-HIS protein pulled down decreased progressively as increasing amounts of MdBT2-HIS protein were added, indicating that MdBT2-HIS competed with GST-$2a^{pol}$ to interact with 1a-HIS in vitro (Figures 7c and S7b). We also observed that MdBT2-HIS was not pulled down by GST-$2a^{pol}$ (Figure 7c), indicating that they did not interact with each other, similar to the results of the Y2H assay (Figure S4). Thus, in addition to promoting 1a ubiquitination and degradation, MdBT2 may also inhibit ApNMV viral genomic RNA replication by interfering with the interaction between viral replication components 1a and $2a^{pol}$.

3 | DISCUSSION

As obligate parasites with a limited genome, plant viruses interact extensively with their hosts to hijack the plant intracellular machinery for multiplication and infection. This may lead to disordered plant physiological responses and the development of visible diseases that compromise plant growth and development. To defend themselves, plants employ multiple strategies to restrict viral infection, including gene silencing, hormone-mediated defence, immune receptor signalling, and protein modification and degradation (Alcaide-Loridan & Jupin, 2012; Calil & Fontes, 2017; Incarbone & Dunoyer, 2013; Korner et al., 2013; Mandadi & Scholthof, 2013). The UPS is a highly conserved protein degradation pathway in eukaryotes and participates in the regulation of many cellular mechanisms, including defence responses against viruses (Alcaide-Loridan & Jupin, 2012; Zhou & Zeng, 2017).

To date, the UPS pathway has been reported to be involved in disrupting different stages of viral infection, such as viral genome replication and movement. For instance, the UPS restricts the

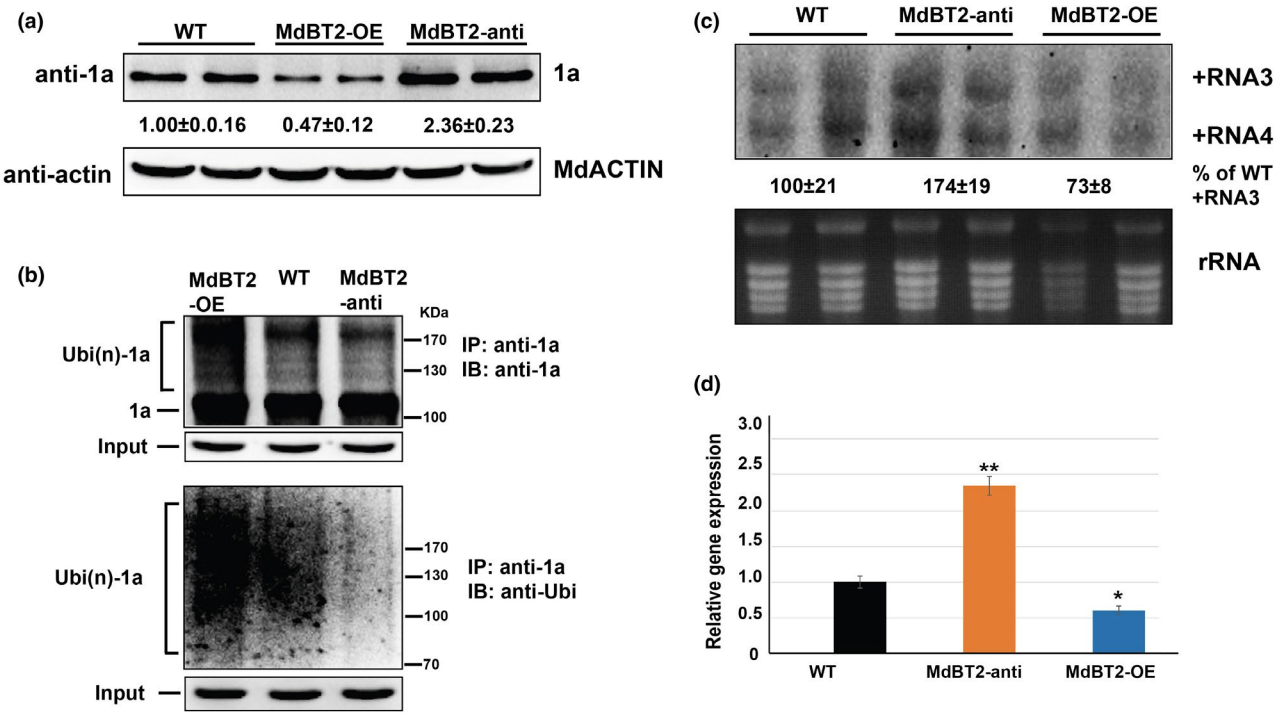

FIGURE 6 MdBT2 inhibits ApNMV genomic RNA replication by promoting the degradation and ubiquitination of viral protein 1a. An infectious clone of ApNMV was agro-infiltrated into leaves of wild type (WT), *MdBT2*-OE (overexpression), and *MdBT2*-anti (antisense), and total proteins (a, b) and RNA (c) were extracted 5 days after infiltration for further investigation. (a) 1a protein level in leaves of WT, *MdBT2*-OE, and *MdBT2*-anti transgenic apple plantlets. Anti-1a specific antibody was used to detect 1a protein. MdACTIN served as a loading control. The values indicate the intensity of bands, and the WT was set to 1.0. (b) MdBT2-mediated 1a protein ubiquitination in vivo. Total proteins were extracted, and anti-1a antibody was used for immunoprecipitation (IP); anti-1a (top panel) and anti-Ubi (bottom panel) antibodies were used for immunoblotting (IB) to detect the target proteins. Input indicates the samples collected before IP and detected with anti-ACTIN antibody. 1a and poly-ubiquitinated 1a (Ubi(n)-1a) are labelled on the left side. Detection of ApNMV genomic RNA accumulation in leaves of WT, *MdBT2*-OE, and *MdBT2*-anti transgenic plantlets was performed via northern blotting (c) and reverse transcription quantitative PCR (RT-qPCR) (d). Total RNA was extracted using the hot phenol method. In the northern blotting assay, digoxygenin (DIG)-labelled probes targeting the coat protein (CP) coding sequence were used to detect the (+)RNA3 and (+)RNA4 of ApNMV. The values indicate the signal intensity of (+)RNA3 and the band intensity of the WT was set to 100%. The rRNA served as a loading control. In RT-qPCR analysis (d), PCR primers targeting CP coding sequence were used and *MdACTIN* served as housekeeping gene. Bars indicate mean values of the relative transcript levels of ApNMV CP-coding gene. The mean values were calculated from nine repeats, for which the whole experiment was repeated three times with three technical replicates each time. Error lines within the bars indicating *SD* of the nine repeats. The mean value of WT was set to 1.0. Significant difference was analysed between the relative transcript levels of the ApNMV CP-coding gene in different transgenic plantlets with that in WT. $^{*}p < 0.05$, $^{**}p < 0.01$ (based on single factor analysis of variance). Representative images of three independent experiments are shown here

replication of turnip yellow mosaic virus (TYMV) by degrading and eliminating its RdRp protein during viral infection of *Arabidopsis* (Camborde et al., 2010; Prod'homme et al., 2001). A recent study showed that an E3 ligase NbUbE3R1 (ubiquitin E3 ligase containing RING domain 1) inhibits the replication of bamboo mosaic virus (BaMV), probably by interacting with the viral replicase (Chen et al., 2019). Here, we found that MdBT2 interacted with and promoted the ubiquitination and degradation of viral protein 1a, which is likely to play an essential role in viral replication based on the known function of the BMV homologous protein (Diaz & Wang, 2014), thereby inhibiting the replication of ApNMV in apple (Figures 3, 4, and 6). Virus movement-related proteins are also potential substrates of the UPS pathway in plant defence responses to control viral infection. For example, the movement protein (MP) of tobacco mosaic virus (TMV) (Reichel & Beachy, 2000), TYMV (Drugeon & Jupin, 2002), and potato leaf roll virus (PLRV) (Vogel et al., 2007) have been reported to be degraded by the UPS pathway. We also investigated the protein interactions between ApNMV MP and MdBT2 to see whether the latter was involved in regulating virus movement, but MdBT2 interacted only with 1a, not with any other viral proteins (Figure S4). Nevertheless, the UPS pathway is one of the common strategies used by plants to defend against virus infection.

BT2 was first identified in a Y2H assay designed to screen for calmodulin-binding proteins (Du & Poovaiah, 2004). It was later found to be involved in the assembly of E3 ligase with CUL3 and RBX1, and was shown to be functional in substrate recognition in the model plant *Arabidopsis* (Figueroa et al., 2005). BT2 was then shown to act downstream of TAC1 to regulate the induction of telomerase

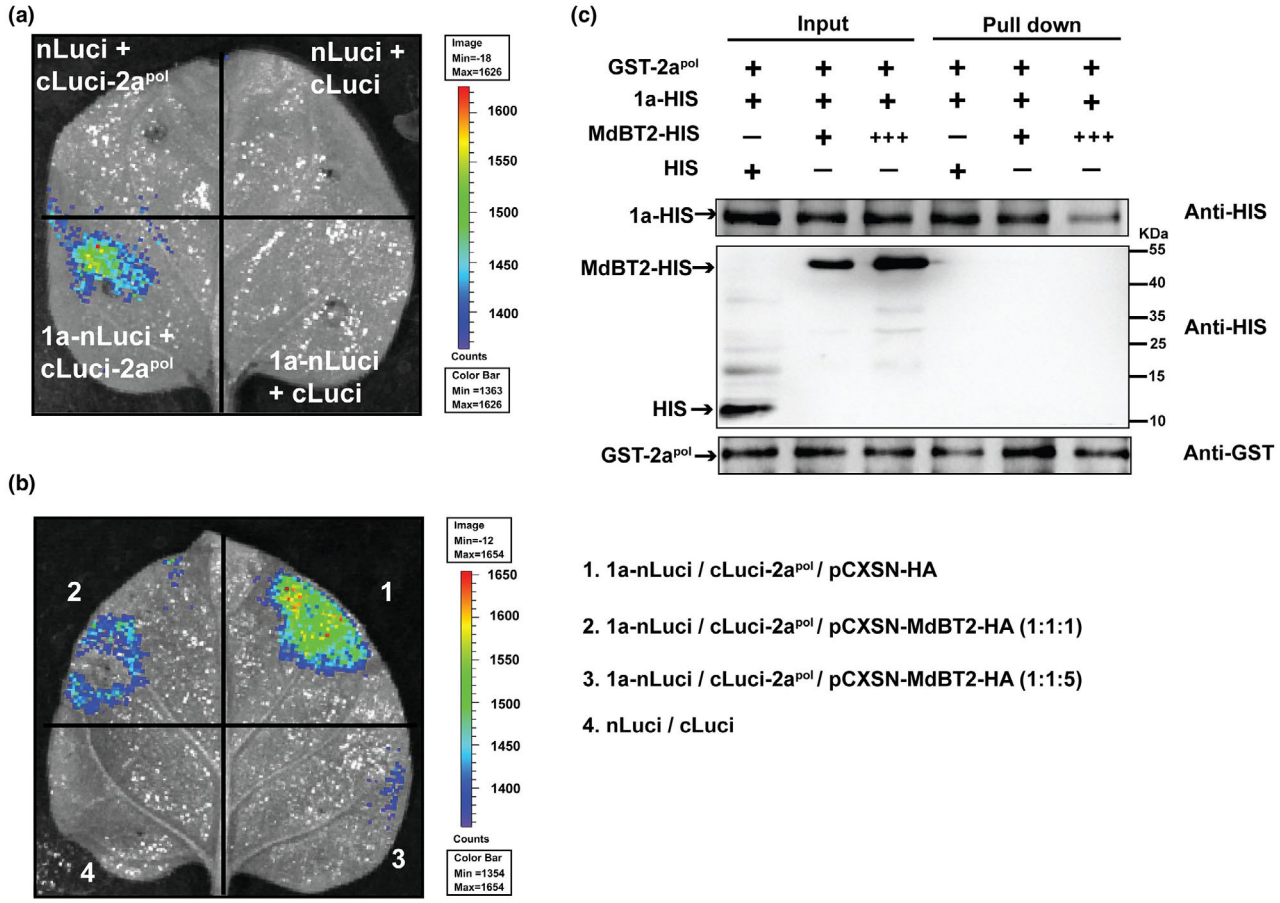

FIGURE 7 MdBT2 interferes with the interaction between 1a and 2a^{pol}. (a) 1a interacts with 2a^{pol} in *Nicotiana benthamiana* cells in a luciferase complementation imaging assay. *Agrobacterium* harbouring different combinations were co-infiltrated into different parts of the same *N. benthamiana* leaf, and the images were taken 3 days after infiltration with an in vivo imaging system after the leaves had been incubated with luciferase substrate in the dark for 3 min. (b) A luciferase complementation imaging assay showed the effect of MdBT2-HA protein on the interaction between 1a and 2a^{pol}. *Agrobacterium* harbouring 1a-nLuci and cLuci-2a^{pol} were mixed and co-infiltrated with *Agrobacterium* containing pCXSN-MdBT2-HA or pCXSN-HA. Increasing ratios of pCXSN-MdBT2-HA were included in the mix, from 1:1:1 (indicating that OD_{600} of the three were the same) to 1:1:5 (indicating that the OD_{600} of pCXSN-MdBT2-HA was five times that of 1a-nLuci and cLuci-2a^{pol}). Different combinations are illustrated on the right side of the image. The bars on the right side of (a) and (b) indicate the intensity of the captured signals. The empty nLuci and cLuci vectors served as controls. (c) A competitive pull-down assay showed the effect of MdBT2-HIS on the interaction between GST-2a^{pol} and 1a-HIS. Equal amounts of GST-2a^{pol} and 1a-HIS were mixed and incubated with different amounts of MdBT2-HIS protein and passed through a glutathione (GSH)-attached column. For the amount of MdBT2-HIS, + indicates 2 μg of protein and + + + indicates 6 μg of protein. A simple HIS-tag protein served as a control when MdBT2-HIS was absent. Anti-HIS antibody was used to detect the 1a-HIS and MdBT2-HIS proteins. All experiments were repeated three times and representative images are shown

(Ren et al., 2007) and to mediate plant responses to nutrients (nitrogen and sugar), hormones (auxin and abscisic acid [ABA]), and stresses (cold and H_2O_2) (Mandadi et al., 2009). BT2 is also a nitrate-responsive protein, and the expression of the BT2-encoding gene is induced by nitrate in both *Arabidopsis* (Mandadi et al., 2009) and apple (Figure S1a). Recent findings suggest that MdBT2 regulates the accumulation of anthocyanin and malate in apple by interacting with and degrading MdMYB1 (Wang et al., 2018), MdCIbHLH1 (Zhang et al., 2020), and MdMYB73 (Zhang et al., 2020) in response to nitrate. Here, we found that nitrate treatment promoted the degradation of viral protein 1a in vitro through the proteasome pathway (Figures 2 and S2). Overexpressing *MdBT2* inhibited viral RNA replication by targeting and degrading viral protein 1a (Figures 4 and 6). These findings imply that a moderate increase in nutrient application may help to control ApNMV infection during apple cultivation.

Moreover, our recent findings demonstrate that MdBT2 plays critical roles in regulating cellular metabolism in response to multiple environmental factors as a subunit of E3 ligase. For example, MdBT2 integrates the signals from ABA, wounding, drought, light, and UV-B to regulate the biosynthesis and accumulation of anthocyanins by targeting and degrading bZIP44 (basic leucine zipper 44) (An et al., 2018), WRKY40 (An, Zhang, You, et al., 2019), ERF38 (ethylene response factor 38) (An, Zhang, et al., 2020), TCP46 (teosinte branched/cycloidea/proliferating 46) (An, Liu, et al., 2020), and BBX22 (B-box 22) (An, Wang et al., 2019). In addition, MdBT2 is reported to regulate leaf senescence through its interactions with

MdbHLH93 (An, Zhang, Bi, et al., 2019), MdMYC2, and MdJAZ2 (JASMONATE ZIM domain 2) (An et al., 2021). Collectively, these findings strongly support that MdBT2 serves as a signal hub to regulate cellular metabolism in response to biotic and abiotic stresses.

MdBT2, a member of the BTB-TAZ subfamily, contains an N-terminal BTB domain, a BACK-like domain in the middle, and a C-terminal TAZ domain. As an adaptor protein in the CRL3 ligase complex, BT2 interacts with both CUL3 and a potential substrate to mediate target protein ubiquitination and degradation (Petroski & Deshaies, 2005). We found that both the BACK-like and TAZ domains were responsible for interacting with ApNMV 1a (Figure 3a). MdBT2 also interacted with MdCUL3A (Figure S6a), as has been shown previously (Wang et al., 2018; Zhao et al., 2016). However, as a possible component of the E3 ligase, MdCUL3A had minimal effect on 1a protein degradation in vitro (Figure 5a), and MdCUL3A even competed with ApNMV 1a to interact with MdBT2 (Figure 5b), indicating that MdBT2 promotes 1a ubiquitination and degradation in an MdCUL3A-independent pathway. In fact, it has also been reported that MdBT2 promotes MdMYB1 degradation in an MdCUL3A-independent pathway in apple (Wang et al., 2018). MdCUL3A-mediated inhibition of the MdBT2–1a interaction should have logically resulted in increased stability of 1a, but we observed a minimal effect on 1a protein degradation in *MdCUL3A*-overexpressing apple callus compared to that of WT (Figure 5a). Two possible reasons may account for this: (a) some other BTB proteins have been reported to interact with non-CUL proteins and function in a CUL3-independent manner (Leljak Levanic et al., 2012; Luke-Glaser et al., 2005). Therefore, MdBT2 may recruit some other, yet unknown, E3 ligase(s) or non-CUL proteins to mediate the ubiquitination and degradation of targets like MdMYB1 and viral 1a protein; (b) MdBT2-mediated UPS is not the only pathway for 1a degradation, and some other cellular protein modification and degradation systems, such as the autophagy-lysosome pathway, sumoylation, and phosphorylation, may also be involved in 1a protein degradation, which need further efforts to verify.

In the well-established model virus BMV, both 1a and $2a^{pol}$ are necessary and sufficient to support viral genome replication, and the 1a–$2a^{pol}$ interactions play a critical role in this process (Diaz & Wang, 2014). Deletion of the N terminus of $2a^{pol}$, which is responsible for its interaction with 1a, severely inhibits BMV viral RNA replication (Kao & Ahlquist, 1992; Traynor et al., 1991). Our previous findings revealed that the C terminus of ApNMV 1a and the N terminus of ApNMV $2a^{pol}$ are required for 1a–$2a^{pol}$ interactions (Zhang, Zhang, et al., 2020). Here, we reported that both the N-terminal MET domain and the C-terminal HEL domain of 1a were required for interaction with MdBT2 (Figure 3b), and increased amounts of MdBT2 interfered with the 1a–$2a^{pol}$ interaction (Figure 7). This may be another reason why ApNMV viral replication was inhibited in *MdBT2*-overexpressing transgenic apple leaves (Figure 6c). In addition, inter- and intramolecular interactions of 1a also play an important role in BMV replication (Diaz et al., 2012), and similar interactions in ApNMV have been verified in our previous reports (Zhang, Zhang, et al., 2020). We therefore predict that the MdBT2–1a interactions would also interrupt the inter- or intramolecular interactions of 1a, leading to restricted viral RNA replication.

Nitrogen is a macronutrient for plant growth and development, and it is also involved in regulating interactions between host plants and pathogens (Dordas, 2008). Based on available nitrogen in the soil, a deficiency or excess of nitrogen may modulate plant resistance through as-yet-unknown mechanisms to counteract pathogens (Huber & Watson, 1974). NO, which is generated in part during nitrate assimilation by nitrate reductase, plays critical roles in plant immunity (Wendehenne et al., 2014). NO was first found to mediate plant defence reactions against bacteria (Delledonne et al., 1998), and it was later demonstrated to activate the hypersensitive reaction to counteract pathogens in tobacco (Asai & Yoshioka, 2009; Kumar & Klessig, 2000). Enhanced NO content has been shown to increase plant resistance to TMV (Klessig et al., 2000), and NO also plays a role in brassinosteroid-mediated resistance against CMV and TMV in plants (Deng et al., 2016; Zou et al., 2018). Feeding tobacco plants with nitrate enhances their resistance to *P. syringae* pv. *phaseolicola* by increasing the accumulation of NO and SA, SA-mediated *PR* gene expression, and polyamine-mediated hypersensitive reactions (Gupta et al., 2013). Here, we found that increased nitrate enabled apple plantlets to inhibit ApNMV genomic RNA replication through MdBT2-mediated ubiquitination and degradation of viral replication protein 1a. Of course, enhanced nitrate may also inhibit ApNMV genomic RNA replication through SA or NO signalling pathways, which is an interesting point and will require further investigation.

In summary, we identified the nitrate-responsive BTB domain-containing protein MdBT2 in apple that inhibits ApNMV viral RNA replication by mediating the degradation of ApNMV 1a protein and interfering with the interactions between viral replication proteins 1a and $2a^{pol}$. Our work reveals the potential role of *MdBT2* as a target gene that may be used for genetic breeding to control apple mosaic disease in apple.

4 | EXPERIMENTAL PROCEDURES

4.1 | Plant materials and growth conditions

Tissue-cultured seedlings of apple (*Malus domestica* 'Royal Gala') GL3 were used in this study (Dai et al., 2013). The *MdBT2*-OE and *MdBT2*-anti transgenic plantlets were generated in our previous work and maintained in our laboratory (Wang et al., 2018). The WT and transgenic GL3 plantlets were grown on Murashige and Skoog (MS) medium supplemented with 0.2 mg/L gibberellin (GA), 0.6 mg/L 6-benzylamino-purine (6-BA), and 0.2 mg/L naphthylacetic acid (NAA) at 25°C under long-day (16 h light/8 h dark) conditions (Wang et al., 2018). The *MdBT2*-OE (pIR-MdBT2-GFP) and *MdBT2*-anti (pIR-MdBT2) transgenic apple calli, as well as the *MdCUL3A* overexpression apple calli, were generated previously and maintained in our laboratory (Wang et al., 2018; Zhao et al., 2016). WT and transgenic Orin apple calli were cultured on MS medium containing 0.4 mg/L 6-BA and 1.5 mg/L (2,4-dichlorophenoxyacetic acid [2,4-D]) at 25°C

under constant dark conditions. *N. benthamiana* plants were maintained in a growth chamber with a 16 h light/8 h dark photoperiod at 23°C.

4.2 | Plasmid construction and *Agrobacterium*-mediated transformation

All PCR-amplified fragments were first inserted into the pEASY-Blunt-Simple (TransGen Biotech) cloning vector and then ligated into expression vectors. The coding sequences of viral proteins and MdBT2 were inserted into pGAD424 and pGBT9 for Y2H assays. The coding sequences of proteins 1a, MdBT2, and $2a^{pol}$ were inserted into pGEX-4T-1 and pET-32a to obtain GST- and HIS-tagged fusion proteins for pull-down assays. For the BiFC assays, the coding sequences of 1a and MdBT2 were inserted into 35S::SPYCE-cYFP and 35S::SPYNE-nYFP to obtain 1a-cYFP and MdBT2-nYFP, respectively (Walter et al., 2004). Similarly, the coding sequences of 1a, MdBT2, and $2a^{pol}$ were inserted into pGreenII 62-SK-nLuc/-cLuc for luciferase complementation imaging assays (Chen et al., 2008). The coding sequences of 1a and MdBT2 were inserted into pCXSN-HA to obtain pCXSN-1a-HA and pCXSN-MdBT2-HA (Chen et al., 2009). The plant binary vectors used in this work were driven by the cauliflower mosaic virus (CaMV) 35S promoter. All the primers used for plasmid construction are listed in Table S1.

The three segments of ApNMV were amplified from the ApNMV-Lw, which we isolated previously (Zhang, Zhang, et al., 2020), and were inserted into a modified pCAMBIA1300 binary vector in which the viral genes were driven by a double 35S promoter.

For *Agrobacterium*-mediated transformation, the appropriate binary constructs were transformed into *Agrobacterium tumefaciens* LBA4404 and cultured in lysogeny broth (LB) medium supplemented with appropriate antibiotics. For ApNMV infectious clone infection into apple leaves, the three components of ApNMV were transformed into *Agrobacterium*, respectively, and then they were combined together to adjust the OD_{600} (optical density at 600 nm) to 0.1 using infection solution (10 mM $MgCl_2$, 10 mM morpholinoethane sulfonic acid [MES], 0.1 mM acetosyringone) for each component. The complex was then co-transformed into apple leaves via the vacuum method. Samples were collected 4 days after treatment and stored in a freezer at −80°C until required for further processing.

4.3 | Analysis of gene expression

Total RNA was extracted from apple shoots of different treatments using an OminiPlant RNA kit (CoWin Biosciences) as per the manufacturer's instructions. The first-strand cDNA was synthesized using the PrimeScript First Strand cDNA Synthesis Kit (TaKaRa) as per the manufacturer's instructions.

Quantitative real-time PCR solutions (20 μl) were assembled by combining the forward and reverse primers (0.25 μM for each), template cDNA (50 ng), and SYBR Green PCR Master Mix (10 μl). The reactions (95°C for 5 min, 95°C for 15 s, 60°C for 1 min for 40 cycles) were performed using the iCycler iQ5 Detection System (Bio-Rad). 18S rRNA served as the internal control. Relative gene expression was calculated using the $2^{-\Delta\Delta Ct}$ method. Three biological replicates were used for each individual experiment. Primers used for RT-qPCR are listed in Table S2.

4.4 | Yeast-two-hybrid assays

The Y2H studies were performed as reported by Wang et al. (2018). In brief, the cDNA library was constructed by the Oebiotech Company using apple skin. The coding sequences of the targets, including viral $2a^{pol}$, MP, and CP, as well as truncated MdBT2 and ApNMV 1a, were amplified and inserted into pGAD424 and pGBT9 vectors. Different combinations of bait and prey constructs were co-transformed into yeast (Y2H Gold; Clontech) and then cultured on synthetic defined (SD) medium lacking leucine (Leu) and tryptophan (Trp) at 28°C for 2–3 days. The yeast colonies were then transferred onto SD medium without Leu, Trp, histidine (His), and adenine (Ade) to assess the interactions between bait and prey proteins.

4.5 | Bimolecular fluorescence complementation assays

The coding sequences of ApNMV 1a and MdBT2 were inserted into the 35S::SPYCE-cYFP and 35S::SPYNE-nYFP vectors (Walter et al., 2004), respectively. The constructs were transformed into *A. tumefaciens* LBA4404 and co-infiltrated into *N. benthamiana* leaves. Yellow fluorescent protein (YFP) signals were observed under a confocal microscope (LSM880; Zeiss) 2 days after infiltration. Different signals were obtained under the "best signal" mode, and images were acquired from single optical sections in the "Frame" mode, with a scan speed of 6 and a scan time of about 10 s.

4.6 | Luciferase complementation imaging assays

Coding sequences of ApNMV 1a and MdBT2 were inserted into pGreenII 62-KS-cLuc and -nLuc vectors (Chen et al., 2008), respectively. The recombinants were transformed into *A. tumefaciens* LBA4404 and co-infiltrated into *N. benthamiana* leaves. Two days after infiltration, luciferase substrate was sprayed onto the leaves, which were then incubated in the dark for 3 min. Bioluminescent signals were detected with an in vivo imaging system (IVIS, Lumina II). In the IVIS acquisition control panel, "Luminescent" was selected as "Imaging mode", and the exposure time was set to 30 s. After photographs were acquired, a colour scale (shown as a colour bar on the right side of the images) was adjusted to improve the image contrast.

For the competitive assay, coding sequences of ApNMV 1a and $2a^{pol}$ were inserted into the pGreenII 62-KS-nLuc and -cLuc vectors as described previously, and the coding sequence of MdBT2 was

inserted into a pCXSN-HA vector (Chen et al., 2009). All constructs were transformed into *A. tumefaciens* LBA4404. The OD_{600} of *Agrobacterium* containing 1a-nLuc and cLuc-$2a^{pol}$ was adjusted to 0.5. It was then combined with different ratios of pCXSN-MdBT2-HA as indicated in Figure 6b and co-infiltrated into *N. benthamiana* leaves. *Agrobacterium* harbouring the pCXSN-HA plasmid served as the control. The images were acquired as previously described.

4.7 | Pull-down analysis

The full-length cDNAs of ApNMV 1a and MdBT2 were amplified and inserted into pGEX-4T-1 and pET-32a vectors, respectively. The constructs were then transformed into *Escherichia coli* BL21 (DE3) to induce the production of GST- and HIS-tagged fusion proteins by treatment with isopropyl β-D-1-thiogalactopyranoside at 28°C for 6 h. The GST-1a and MdBT2-HIS fusion proteins were premixed for 1 h at 4°C with gentle shaking. The protein mix was combined with GSH-conjugated beads (BEAVER) and then incubated at 4°C for 1 h with gentle shaking. After washing the beads five times to remove nonspecific proteins, bound proteins were eluted from the magnetically separated agarose beads with GSH solution and boiled for 5 min. The supernatant was then used for sodium dodecyl sulphate-polyacrylamide gel electrophoresis (SDS-PAGE) and immunoblotted with specific antibodies.

For competitive pull-down assays, equal amounts (2 μg) of GST-$2a^{pol}$ and 1a-HIS were mixed with HIS tag protein (2 μg, none is fused to the HIS tag and serves as a control) or different concentrations (2 and 6 μg) of MdBT2-HIS fusion protein, then premixed at 4°C for 1 h with gentle shaking. Following the previously described protocol for pull-down assays, the bound proteins were resuspended in GSH solution, separated by SDS-PAGE, and detected by immunoblotting with anti-GST (Abmart) and anti-HIS (Abmart) antibodies.

4.8 | Protein extraction and western blotting

The total proteins were extracted from apple tissues, including calli and leaves, using protein extraction solution (100 mM Tris-HCl [pH 7.5], 1 mM ethylenediaminetetraacetic acid disodium salt, 1% polyvinylpyrrolidone K30, 0.07% β-mercaptoethanol, and 6.85% sucrose). Prepared protein samples were separated on a 10% gel using SDS-PAGE and transferred to polyvinylidene difluoride membranes (Roche). Specific antibodies were applied to detect corresponding proteins, and peroxidase-conjugated secondary antibodies (Adcam) were used to visualize the immunoreactive proteins with an ECL detection kit (Millipore). MdACTIN was used as the loading control.

4.9 | Co-immunoprecipitation assays

Co-immunoprecipitation assays were performed using the BeaverBeads protein A/G immunoprecipitation kit (BEAVER Biomedical Engineering) per the manufacturer's protocol. In brief, the beads and antibodies were pretreated with the binding buffer supplied in the kit, and the extracted total protein was then mixed with the pretreated antibodies and beads, and incubated overnight at 4°C with gentle shaking. After washing five times, the beads were separated using a magnet and resuspended in elution buffer containing Coomassie Brilliant blue. The precipitates were boiled for 5 min and separated by SDS-PAGE for further analysis.

4.10 | Ubiquitination assays

To detect ubiquitinated ApNMV 1a in vivo, *Agrobacterium* harbouring the pCXSN-1a-HA construct or the ApNMV infectious clone was transformed into leaves of WT, *MdBT2*-OE, and *MdBT2*-anti apple by the vacuum technique. The leaves were maintained on MS medium for 5 days and then collected for protein extraction after treatment with 50 μM MG132 for 10 h. The total protein was immunoprecipitated using anti-HA antibody (Abmart) or anti-1a specific antibody with the BeaverBeads protein A/G immunoprecipitation kit (BEAVER Biomedical Engineering) as per the manufacturer's protocol. The precipitates were used for western blotting, and anti-HA, anti-1a, and anti-Ubi (Sigma-Aldrich) antibodies were used to detect the target proteins as described previously.

To detect the ubiquitinated ApNMV 1a in vitro, total protein was first extracted from *35S::MdBT2-GFP* transgenic apple calli pretreated with 50 μM MG132 for 10 h. Then MdBT2-GFP active proteins were precipitated with anti-GFP antibody (Abmart) using BeaverBeads protein A/G immunoprecipitation kit (BEAVER Biomedical Engineering) as per the manufacturer's protocol, as described previously (Zhang, Gu, Cheng, et al., 2020). The ApNMV 1a-HIS protein obtained from the prokaryotic expression system was incubated with or without MdBT2-GFP active proteins in incubation buffer at 30°C for 12 h. The incubation buffer consisted of 50 mM Tris (pH 7.5), 2 mM dithiothreitol (DTT), 50 mM $MgCl_2$, 2 mM ATP, 100 ng human E1 (recombinant human His6 UBE1; BostonBiochem), 100 ng human E2 (recombinant human UbcH5b/UBE2D2, BostonBiochem), and 1 μg ubi (recombinant human Myc Ubiquitin; BostonBiochem). Ubiquitination of the target protein was detected using anti-HIS (Abmart) and anti-Ubi (Sigma-Aldrich) antibodies.

4.11 | Cell-free degradation assays

1a-HIS protein was obtained from a prokaryotic expression system using *E. coli* BL21 (DE3). Total proteins were extracted from apple calli using degradation buffer: 25 mM Tris-HCl (pH 7.5), 10 mM NaCl, 10 mM $MgCl_2$, 5 mM DTT, 10 mM ATP, and 4 mM phenylmethysulfonyl fluoride (Wang et al., 2009). The concentrations of collected protein supernatants and 1a-HIS were measured using the Bradford reagent (Bio-Rad). Then, 100 ng of 1a-HIS protein and 300 ng of total protein were mixed and incubated at 22°C for the indicated time. For the proteasome inhibition assay, the mixed proteins were pretreated with the proteasome inhibitor MG132 (50 μM, stock solution

is prepared with 0.5% DMSO) for 30 min, and DMSO served as the mock control. The protein mixture was collected at the indicated time points, and the reactions were stopped with SDS-PAGE loading buffer and boiled for 5 min. The samples were then applied to western blotting assays for protein degradation analysis. The results were quantified using Quantity One 1-D Analysis software (Bio-Rad).

4.12 | RNA extraction and northern blotting

Total RNA was extracted for northern blotting using the hot phenol method (Kohrer & Domdey, 1991). Equal amounts (15 μg) of RNA were used for electrophoresis and transferred to nylon membranes. DIG-labelled probes targeting the CP-coding sequence of ApNMV were generated and used for hybridization to detect the positive-strand (+) RNA3 and (+)RNA4 per the manufacturer's protocol (Roche). Anti-DIG antibody (conjugated with alkaline phosphatase; Roche) was used for immunoblotting, and a chemiluminescent substrate for alkaline phosphatase was used for imaging with a gel imager (Bio-Rad).

ACKNOWLEDGEMENTS

This study was financially supported by the National Natural Science Foundation of China (31901988), the China Postdoctoral Science Foundation (2019M662413, 2020T130388), and Shandong Postdoctoral Innovation Project (201902042).

AUTHOR CONTRIBUTIONS

Z.Z., X.F.W., and Y.J.H. initiated and designed the research. Z.Z., F.J.Z., P.S., P.F.Z., and Y.H.X. performed the experiments. Z.Z. and Y.J.H. analysed the data. Z.Z. and Y.J.H. wrote and revised the manuscript. C.X.Y. and Y.J.H. supervised the project.

DATA AVAILABILITY STATEMENT

The data that support the findings of this study are available in the Supporting Information of this article.

REFERENCES

Adams, E.H.G. & Spoel, S.H. (2018) The ubiquitin–proteasome system as a transcriptional regulator of plant immunity. *Journal of Experimental Botany*, 69, 4529–4537.

Alcaide-Loridan, C. & Jupin, I. (2012) Ubiquitin and plant viruses, let's play together! *Plant Physiology*, 160, 72–82.

An, J.-P., Wang, X.-F., Zhang, X., You, C.-X. & Hao, Y. (2021) Apple MdBT2 protein negatively regulates jasmonic acid-triggered leaf senescence by modulating the stability of MYC2 and JAZ2. *Plant, Cell & Environment*, 44, 216–233.

An, J.-P., Yao, J.-F., Xu, R.-R., You, C.-X., Wang, X.-F. & Hao, Y.-J. (2018) Apple bZIP transcription factor MdbZIP44 regulates abscisic acid-promoted anthocyanin accumulation. *Plant, Cell and Environment*, 41, 2678–2692.

An, J.-P., Zhang, X., Bi, S., You, C.-X., Wang, X.-F. & Hao, Y. (2019) MdbHLH93, an apple activator regulating leaf senescence, is regulated by ABA and MdBT2 in antagonistic ways. *New Phytologist*, 222, 735–751.

An, J.-P., Zhang, X., You, C.-X., Bi, S., Wang, X.-F. & Hao, Y. (2019) MdWRKY40 promotes wounding-induced anthocyanin biosynthesis in association with MdMYB1 and undergoes MdBT2-mediated degradation. *New Phytologist*, 224, 380–395.

An, J.-P., Wang, X.-F., Zhang, X., Bi, S., You, C.-X. & Hao, Y. (2019) MdBBX22 regulates UV-B-induced anthocyanin biosynthesis through regulating the function of MdHY5 and is targeted by MdBT2 for 26 proteasome-mediated degradation. *Plant Biotechnology Journal*, 17, 2231–2233.

An, J.-P., Wang, X.-F. & Hao, Y. (2020) BTB/TAZ protein MdBT2 integrates multiple hormonal and environmental signals to regulate anthocyanin biosynthesis in apple. *Journal of Integrative Plant Biology*, 62, 1643–1646.

An, J.-P., Zhang, X., Bi, S., You, C.-X., Wang, X.-F. & Hao, Y. (2020) The ERF transcription factor MdERF38 promotes drought stress-induced anthocyanin biosynthesis in apple. *The Plant Journal*, 101, 573–589.

An, J.-P., Liu, Y.-J., Zhang, X.-W., Bi, S.-Q., Wang, X.-F., You, C.-X. et al. (2020) Dynamic regulation of anthocyanin biosynthesis at different light intensities by the BT2-TCP46-MYB1 module in apple. *Journal of Experimental Botany*, 71, 3094–3109.

Asai, S. & Yoshioka, H. (2009) Nitric oxide as a partner of reactive oxygen species participates in disease resistance to necrotrophic pathogen *Botrytis cinerea* in *Nicotiana benthamiana*. *Molecular Plant-Microbe Interactions*, 22, 619–629.

Bachmair, A., Novatchkova, M., Potuschak, T. & Eisenhaber, F. (2001) Ubiquitylation in plants: a post-genomic look at a post-translational modification. *Trends in Plant Science*, 6, 463–470.

Bujarski, J., Figlerowicz, M., Gallitelli, D., Roossinck, M. & Scott, S. (2012) Family *Bromoviridae*. In: King, A., Adams, M., Carstens, E. & Lefkowitz, E. (Eds.) *Virus Taxonomy, Ninth Report of the International Committe on Taxonomy of Viruses*. London: Academic Press, pp. 965–976.

Calil, I. & Fontes, E. (2017) Plant immunity against viruses: antiviral immune receptors in focus. *Annuals of Botany*, 119, 711–723.

Camborde, L., Planchais, S., Tournier, V., Jakubiec, A., Drugeon, G., Lacassagne, E. et al. (2010) The ubiquitin-proteasome system regulates the accumulation of turnip yellow mosaic virus RNA-dependent RNA polymerase during viral infection. *The Plant Cell*, 22, 3142–3152.

Chen, H., Zou, Y., Shang, Y., Lin, H., Wang, Y., Cai, R. et al. (2008) Firefly luciferase complementation imaging system assay for protein–protein interactions in plants. *Plant Physiology*, 146, 368–376.

Chen, I.-H., Chang, J.-E., Wu, C.-Y., Huang, Y.-P., Hsu, Y.-H. & Tsai, C.-H. (2019). An E3 ubiquitin ligase from *Nicotiana benthamiana* targets the replicase of bamboo mosaic virus and restricts its replication. *Molecular Plant Pathology*, 20, 673–684.

Chen, S., Songkumarn, P., Liu, J. & Wang, G. (2009) A versatile zero background T-vector system for gene cloning and functional genomics. *Plant Physiology*, 150, 1111–1121.

Dai, H., Li, W., Han, G., Yang, Y.I., Ma, Y., Li, H.E. et al. (2013) Development of a seedling clone with high regeneration capacity and susceptibility to *Agrobacterium* in apple. *Scientia Horticulturae*, 164, 202–208.

Delledonne, M., Xia, Y., Dixon, R.A. & Lamb, C. (1998) Nitric oxide functions as a signal in plant disease resistance. *Nature*, 394, 585–588.

Deng, X., Zhu, T., Zou, L., Han, X., Zhou, X., Xi, D. et al. (2016) Orchestration of hydrogen peroxide and nitric oxide in brassinosteroid-mediated systemic virus resistance in *Nicotiana benthamiana*. *The Plant Journal*, 85, 478–493.

Diaz, A., Gallei, A. & Ahlquist, P. (2012) Bromovirus RNA replication compartment formation requires concerted action of 1a's self-interacting RNA capping and helicase domains. *Journal of Virology*, 86, 821–834.

Diaz, A. & Wang, X. (2014) Bromovirus-induced remodeling of host membranes during viral RNA replication. *Current Opinion in Virology*, 9, 104–110.

Dordas, C. (2008) Role of nutrients in controlling plant diseases in sustainable agriculture. A review. *Agronomy for Sustainable Development*, 28, 33–46.

Drugeon, G. & Jupin, I. (2002) Stability in vitro of the 69K movement protein of turnip yellow mosaic virus is regulated by the ubiquitin-mediated proteasome pathway. *Journal of General Virology*, 83, 3187–3197.

Du, L. & Poovaiah, B. (2004) A novel family of Ca^{2+}/calmodulin-binding proteins involved in transcription regulation: interaction with fsh/Ring3 class transcription activatiors. *Plant Molecular Biology*, 54, 549–569.

Figueroa, P., Gusmaroli, G., Serino, G., Habashi, J., Ma, L., Shen, Y. et al. (2005) *Arabidopsis* has two redundant Cullin3 proteins that are essential for embryo development and that interact with RBX1 and BTB proteins to form multisubunit E3 ubiquitin ligase complexes in vivo. *The Plant Cell*, 17, 1180–1195.

Genschik, P., Sumara, I. & Lechner, E. (2013) The emerging family of CULLIN3-RING ubiquitin ligases (CRL3s): cellular functions and disease implications. *EMBO Journal*, 32, 2307–2320.

Gingerich, D.J., Gagne, J.M., Salter, D.W., Hellmann, H., Estelle, M., Ma, L. et al. (2005) Cullins 3a and 3b assemble with members of the broad complex/tramtrack/bric-a-brac (BTB) protein family to form essential ubiquitin-protein ligases (E3s) in *Arabidopsis*. *Journal of Biological Chemistry*, 280, 18810–18821.

Gupta, K.J., Brotman, Y., Segu, S., Zeier, T., Zeier, J., Persijn, S.T. et al. (2013) The form of nitrogen nutrition affects resistance against *Pseudomonas syringae* pv. *phaseolicola* in tobacco. *Journal of Experimental Botany*, 64, 553–568.

Han, P.-L., Wang, C.-K., Liu, X.-J., Dong, Y.-H., Jiang, H., Hu, D.-G. et al. (2019) BTB-BACK domain E3 ligase MdPOB1 suppresses plant pathogen defense against *Botryosphaeria dothidea* by ubiquitinating and degrading MdPUB29 protein in apple. *Plant and Cell Physiology*, 60, 2129–2140.

Ho, C., Lin, S., Hu, H. & Tsay, Y. (2009) CHL1 functions as a nitrate sensor in plants. *Cell*, 138, 1184–1194.

Hotton, S. & Callis, J. (2008) Regulation of cullin RING ligases. *Annual Review of Plant Biology*, 59, 467–489.

Hua, Z. & Vierstra, R.D. (2011) The cullin-RING ubiquitin-protein ligases. *Annual Review of Plant Biology*, 62, 299–334.

Huber, D.M. & Watson, R.D. (1974) Nitrogen form and plant disease. *Annual Review of Phytopathology*, 12, 139–165.

Incarbone, M. & Dunoyer, P. (2013) RNA silencing and its suppression: novel insights from in planta analysis. *Trends in Plant Science*, 18, 382–392.

Kao, C.C. & Ahlquist, P. (1992) Identification of the domains required for direct interaction of the helicase-like and polymerase-like RNA replication proteins of brome mosaic virus. *Journal of Virology*, 66, 7293–7302.

Klessig, D.F., Durner, J., Noad, R., Navarre, D.A., Wendehenne, D., Kumar, D. et al. (2000) Nitric oxide and salicylic acid signaling in plant defense. *Proceedings of the National Academy of Sciences of the United States of America*, 97, 8849–8855.

Kohrer, K. & Domdey, H. (1991) Preparation of high molecular weight RNA. *Methods in Enzymology*, 194, 398–405.

Korner, C., Klause, D., Niehl, A., Dominguez-Ferreras, A., Chinchilla, D., Boller, T. et al. (2013) The immunity regulator BAK1 contributes to resistance against diverse RNA viruses. *Molecular Plant-Microbe Interactions*, 26, 1271–1280.

Kumar, D. & Klessig, D.F. (2000) Differential induction of tobacco MAP kinases by the defense signals nitric oxide, salicylic acid, ethylene, and jasmonic acid. *Molecular Plant-Microbe Interactions*, 13, 347–351.

Kunz, S., Gardeström, P., Pesquet, E. & Kleczkowski, L.A. (2015) Hexokinase 1 is required for glucose-induced repression of bZIP63, At5g22920, and BT2 in *Arabidopsis*. *Frontiers in Plant Science*, 6, 525.

Leljak Levanic, D., Horvat, T., Martincic, J. & Bauer, N. (2012) A novel bipartite nuclear localization signal guides BPM1 protein to nucleolus suggesting its Cullin3 independent function. *PLoS One*, 7, e51184.

Luke-Glaser, S., Pintard, L., Lu, C., Mains, P.E. & Peter, M. (2005) The BTB protein MEL-26 promotes cytokinesis in *C. elegans* by a CUL-3-independent mechanism. *Current Biology*, 15, 1605–1615.

Mandadi, K.K., Misra, A., Ren, S. & McKnight, T.D. (2009) BT2, a BTB protein, mediates multiple responses to nutrients, stresses, and hormones in *Arabidopsis*. *Plant Physiology*, 150, 1930–1939.

Mandadi, K.K. & Scholthof, K.-B. (2013) Plant immune responses against viruses: how does a virus cause disease? *The Plant Cell*, 25, 1489–1505.

Mazzucotelli, E., Belloni, S., Marone, D., De Leonardis, A., Guerra, D., Di Fonzo, N. et al. (2006) The e3 ubiquitin ligase gene family in plants: regulation by degradation. *Current Genomics*, 7, 509–522.

Metzger, M., Pruneda, J., Klevit, R. & Weissman, A. (2014) RING-type E3 ligases: master manipulators of E2 ubiquitin-conjugating enzymes and ubiquitination. *Biochimica et Biophysica Acta*, 1843, 47–60.

Misra, A., McKnight, T.D. & Mandadi, K.K. (2018) Bromodomain proteins GTE9 and GTE11 are essential for specific BT2-mediated sugar and ABA responses in *Arabidopsis thaliana*. *Plant Molecular Biology*, 96, 393–402.

Noda, H., Yamagishi, N., Yaegashi, H., Xing, F., Xie, J., Li, S. et al. (2017) Apple necrotic mosaic virus, a novel ilarvirus from mosaic-diseased apple trees in Japan and China. *Journal of General Plant Pathology*, 83, 83–90.

Orosa, B., He, Q., Mesmar, J., Gilroy, E., McLellan, H., Yang, C. et al. (2017) BTB-BACK domain protein POB1 suppresses immue cell death by targeting ubiquitin E3 ligase PUB17 for degradation. *PLoS Genetics*, 13, e1006540.

Petroski, M. & Deshaies, R. (2005) Function and regulation of cullin-RING ubiquitin ligases. *Nature Review of Molecular Cell Biology*, 6, 9–20.

Prod'homme, D., Le Panse, S., Drugeon, G. & Jupin, I. (2001) Detection and subcellular localization of the turnip yellow mosaic virus 66K replication protein in infected cells. *Virology*, 281, 88–101.

Reichel, C. & Beachy, R. (2000) Degradation of tobacco mosaic virus movement protein by the 26S proteasome. *Journal of Virology*, 74, 3330–3337.

Ren, S., Mandadi, K.K., Boedeker, A.L., Rathore, K.S. & McKnight, T.D. (2007) Regulation of telomerase in Arabidopsis by BT2, an apparent target of TELOMERASE ACTIVATOR1. *The Plant Cell*, 19, 23–31.

Scheible, W.-R., Morcuende, R., Czechowski, T., Fritz, C., Osuna, D., Palacios-Rojas, N. et al. (2004) Genome-wide reprogramming of primary and secondary metabolism, protein synthesis, cellular growth processes, and the regulatory infrastructure of *Arabidopsis* in response to nitrogen. *Plant Physiology*, 136, 2483–2499.

Traynor, P., Young, B. & Ahlquist, P. (1991) Deletion analysis of brome mosaic virus 2a protein: effects on RNA replication and systemic spread. *Journal of Virology*, 65, 2807–2815.

Vierstra, R.D. (2009) The ubiquitin-26S proteasome system at the nexus of plant biology. *Nature Reviews Molecular Cell Biology*, 10, 385–397.

Vogel, F., Hofius, D. & Sonnewald, U. (2007) Intracellular trafficking of potato leafroll virus movement protein in transgenic *Arabidopsis*. *Traffic*, 8, 1205–1214.

Walter, M., Chaban, C., Schütze, K., Batistic, O., Weckermann, K., Näke, C. et al. (2004) Visualization of protein interactions in living plant cells using bimolecular fluorescence complementation. *The Plant Journal*, 40, 428–438.

Wang, F., Zhu, D., Huang, X., Li, S., Gong, Y., Yao, Q. et al. (2009) Biochemical insights on degradation of *Arabidopsis* DELLA proteins gained from a cell-free assay system. *The Plant Cell*, 21, 2378–2390.

Wang, X.-F., An, J.-P., Liu, X., Su, L., You, C.-X. & Hao, Y. (2018) The nitrate-responsive protein MdBT2 regulates anthocyanin biosynthesis by interacting with the MdMYB1 transcription factor. *Plant Physiology*, 178, 890–906.

Wendehenne, D., Gao, Q., Kachroo, A. & Kachroo, P. (2014) Free radical-mediated systemic immunity in plants. *Current Opinion in Plant Biology*, 20C, 127–134.

Wendehenne, D., Lamotte, O., Frachisse, J.M., Barbier-Brygoo, H. & Pugin, A. (2002) Nitrate efflux is an essential component of the cryptogein signaling pathway leading to defense responses and hypersensitive cell death in tobacco. *The Plant Cell*, 14, 1937–1951.

Xing, F., Robe, B.L., Zhang, Z., Wang, H. & Li, S. (2018) Genomic analysis, sequence diversity, and occurrence of apple necrotic mosaic virus, a novel ilarvirus associated with mosaic disease of apple trees in China. *Plant Disease*, 102, 1841–1847.

Zhang, Q.-Y., Gu, K.-D., Cheng, L., Wang, J.-H., Yu, J.-Q., Wang, X.-F. et al. (2020) BTB-TAZ domain protein MdBT2 modulates malate accumulation and vacuolar acidification in response to nitrate. *Plant Physiology*, 183, 750–764.

Zhang, Q., Gu, K., Wang, J., Yu, J., Wang, X.-F., Zhang, S., et al. (2020). BTB-BACK-TAZ domain protein MdBT2-mediated MdMYB73 ubiquitination negatively regulates malate accumulation and vacuolar acidification in apple. *Horticulture Research*, 7, 151.

Zhang, Z., Zhang, F., Zheng, P., Xie, Y., You, C.-X. & Hao, Y. (2020) Determination of protein interactions among replication components of apple necrotic mosaic virus. *Viruses*, 12, 474.

Zhao, Q., Ren, Y., Wang, Q., You, C.-X. & Hao, Y. (2016) Ubiquitination-related MdBT scaffold protein target a bHLH transcription factor for iron homeostasis. *Plant Physiology*, 173, 1973–1988.

Zhou, B. & Zeng, L. (2017) Conventional and unconventional ubiquitination in plant immunity. *Molecular Plant Pathology*, 18, 1313–1330.

Zou, L., Deng, X., Zhang, L., Zhu, T., Tan, W., Muhammad, A. et al. (2018) Nitric oxide as a signaling molecule in brassinosteroid-mediated virus resistance to cucumber mosaic virus in *Arabidopsis thaliana*. *Physiologia Plantarum*, 163, 196–210.

SUPPORTING INFORMATION

Additional supporting information may be found in the online version of the article at the publisher's website.

How to cite this article: Zhang, Z., Xie, Y.-H., Sun, P., Zhang, F.-J., Zheng, P.-F., Wang, X.-F., et al. (2022) Nitrate-inducible MdBT2 acts as a restriction factor to limit apple necrotic mosaic virus genome replication in *Malus domestica*. *Molecular Plant Pathology*, 23, 383–399. https://doi.org/10.1111/mpp.13166